J. Fluid Mech. (1998), *vol.* 370, *pp.* 347–380. Printed in the United Kingdom

An axisymmetric 'fluidic' nozzle to generate jet precession

By G. J. NATHAN, S. J. HILL AND R. E. LUXTON

Department of Mechanical Engineering, The University of Adelaide, Adelaide 5005, Australia

(Received 3 December 1996 and in revised form 14 April 1998)

A continuously unstable precessing flow within a short cylindrical chamber following a large sudden expansion is described. The investigation relates to a nozzle designed to produce a jet which achieves large-scale mixing in the downstream field. The inlet flow in the plane of the sudden expansion is well defined and free from asymmetry. Qualitative flow visualization in water and semi-quantitative surface flow visualization in air are reported which identify this precession within the chamber. Quantitative simultaneous measurements from fast-response pressure transducers at four tapping points on the internal walls of the nozzle chamber confirm the presence of the precessing field. The investigation focuses on the flow within the nozzle chamber rather than that in the emerging jet, although the emerging flow is also visualized.

Two flow modes are identified: a 'precessing jet' mode which is instantaneously highly asymmetric, and a quasi-symmetric 'axial jet' mode. The precessing jet mode, on which the investigation concentrates, predominates in the geometric configuration investigated here. A topologically consistent flow field, derived from the visualization and from the fluctuating pressure data, which describes a three-dimensional and time-dependent precessing motion of the jet within the chamber is proposed. The surface flow visualization quantifies the axial distances to lines of positive and negative bifurcation allowing comparison with related flows involving large-scale precession or flapping reported by others. The Strouhal numbers (dimensionless frequencies) of these flows are shown to be two orders of magnitude lower than that measured in the shear layer of the jet entering the chamber. The phenomenon is demonstrated to be unrelated to acoustic coupling.

1. Introduction

1.1. *Background*

Various methods of jet excitation have been investigated widely, usually with a view to stimulating increased rates of mixing. The means of excitation include acoustic (Hill & Greene 1977), fluidic (Piatt & Viets 1979) and mechanical (Simmons, Lai & Platzer 1981) techniques. Described here is the flow within a nozzle that generates a precessing jet flow which has proved beneficial in combustion applications. Jet precession, as distinct from a swirling motion, refers to the rotation of the jet about an axis other than its own axis. The precession of a jet is generated here by a flow instability downstream from a large sudden expansion and within an axisymmetric chamber which forms part of a 'fluidic' nozzle. The jet flow issuing from this nozzle has been shown to increase the scale of the dominant fluid structures in open gas flames relative to those in a simple jet flame, so that the number of these large

structures present at any one instant within the visible flame is comparably smaller. Newbold, Nathan & Luxton (1997) identified only three of these large structures within an open precessing jet flame compared with the eight typical in a simple jet flame. A fundamental study of the effect of jet precession on combustion has shown that it can be used to increase flame luminosity in and reduce global NO_x emissions from open natural-gas flames (Nathan, Turns & Bandaru, 1996). Nathan, Luxton & Smart (1992) have shown, in a 2 MW test furnace, that the flame generated by a nozzle similar to the one currently under investigation, firing natural gas, generates about one half of the NO_x emissions of an equivalent swirl burner. Flame stability is also increased relative to a conventional free jet (Nathan & Luxton 1988, 1991).

The large-scale (azimuthal) precession of an asymmetric reattaching flow within an axisymmetric chamber appears to have been observed first by Hallett & Gunther (1984). Their apparatus, designed to model the cold flow within a dump combustor, used a diametral expansion ratio of $D/d = 2.2$ with a swirling motion imparted to the flow upstream from the expansion. Here D is the diameter of the chamber into which the jet expands and d is the diameter of the inlet to the chamber. Dellenback, Metzger & Neitzel (1988) examined the influence of the swirl number, a dimensionless ratio of the axial flux of angular momentum to the axial momentum divided by a characteristic diameter, on the class of flow produced in a facility with a diametral expansion ratio of $D/d = 1.94$. They found that the precessing asymmetric instability is generated when the swirl number of the upstream flow is less than that required to produce a central recirculation zone. In this 'low' swirl number regime, they found the sense of the precession to be the opposite of that of the swirl, while at higher swirl numbers associated with the establishment of the central recirculation zone, a vortex core precesses in the same direction as the swirl. They also noted that the flow field is extremely complicated and so limited their experiments to those which characterize broad features of the flow. Independently Luxton & Nathan (1989) studied precession in nozzle configurations with diametral expansion ratios, $D/d \geqslant 3$. They showed that upstream swirl is not a pre-requisite for the generation of a precessing flow instability. Their flow visualization suggested that the reattachment distance associated with the precessing asymmetrical 'jet-like' flow within a chamber is considerably shorter than the reattachments through smaller expansions. These findings are in broad agreement with the measurements of Lipstein (1962) who used mean wall static pressure measurements and Pitot tube traverses to investigate flow through sudden axisymmetric expansions in long round ducts. Lipstein (1962) found that a normalized reattachment distance is constant for $D/d < 3.3$, but decreases with larger expansion ratios. He also deduced that the ratio of the length of the potential core to the reattachment distance is physically significant in determining the reattachment length. However, his experimental techniques were not capable of resolving unsteady flow phenomena and he did not observe flow precession. More recent work by Hill, Nathan & Luxton (1995) has identified the precession of a reattaching flow following a large sudden expansion in a long axisymmetric pipe. No upstream swirl was used in that study. Thus it is apparent that swirl is not a prerequisite for precession provided that the expansion ratio is sufficiently large.

Analogous low-frequency measurements associated with gross motions of a planar jet within a chamber have also been reported. Shakouchi (1981,1989) has conducted measurements in a two-dimensional fluidic oscillator in which the flapping motion is produced when a rectangular jet expands into a short planar chamber. (For the planar case the width of the nozzle at the chamber inlet must be less than the width of the chamber in order for the flapping to occur. This enables flow to pass around the sides

of the reattaching jet.) With an expansion ratio of the jet into the chamber of $D/d = 8$ and a jet inlet Reynolds number $Re_d = 25\,600$, the Strouhal number of the flapping oscillation was found to be $St_{f,d} = f_f d/\bar{u} \approx 2\times10^{-3}$, where f_f is the flapping frequency, d is the width of the planar jet which enters the chamber (D) and $\bar{u}$ is its bulk mean velocity at entry. Likewise in a full Navier–Stokes numerical simulation of a laminar planar jet expanding into a confined planar channel, Battaglia *et al.* (1997) predicted a similar flapping motion with expansion ratios of $D/d = 5$ and 7. They calculated the Strouhal number of the flapping motion to be $7.5 \times 10^{-3} < St_{f,d} < 10 \times 10^{-3}$ for Reynolds numbers in the range $100 < Re < 1000$. That these Strouhal numbers are of the same order of magnitude as those found in precessing flows, namely $St_{p,d} \approx 2 \times 10^{-3}$, suggests that the flows may be related.

The existence of precessing flows in cylindrical chambers and flapping flows in planar chambers, each occurring downstream from a large sudden expansion, have been reported for a wide variety of geometric and flow conditions. However the above experimental studies on precessing flows have not provided sufficiently comprehensive descriptions of the precessing flow itself or of the precision of the apparatus and of the inlet flow conditions to exclude the possibility that the phenomenon is an artifice of some asymmetry within inlet flow or the apparatus. Nathan (1988) conducted a parametric investigation of characteristic chamber dimensions to ascertain, in a semi-quantitative fashion, which ratios of chamber dimensions used in a fluid nozzle favour the formation of a precessing flow mode. Hill, Nathan & Luxton (1992) quantified the geometric configurations which favour precession. However these investigations leave some unanswered questions regarding the influence of asymmetries (even relatively minor ones) in the flow upstream from the nozzle chamber and hence on their significance in the establishment of the precession. None of the above studies gives a sufficiently detailed description of the inlet flow conditions to resolve this issue. Nathan (1988) tested for flow symmetry in the mean velocity profiles at the exit of a large diffuser upstream from the nozzle chamber used in much of his investigation. However the five pipe diameters between the diffuser and the chamber are insufficient to ensure fully developed pipe flow at the inlet to the chamber. Likewise, although several flow path arrangements were studied by Nathan (1988), Nathan & Luxton (1992*a*, *b*) and Hill *et al.* (1992), the focus was on the phenomenon of the precession and no fully definitive set of data describing the inlet conditions and their influence on the precession was presented. The present experimental study has been designed to address this question.

The geometric configurations investigated in the present paper are restricted to the dimensions of the fluidic precessing jet (FPJ) nozzle shown in figure 1(*a*), the arrangement of which is disclosed in a family of patents filed by Luxton, Nathan & Luminis Pty. Ltd. (1991) which have found application in burner designs. Great care has been taken in the present study to ensure that the flow immediately upstream from the chamber (figure 1*b*) is axisymmetric and closely approaches fully developed pipe flow, and that the inlet flow conditions and the details of the apparatus geometry are quantified. The character of the precessing flow is described with the aid of flow visualization and is quantified by data from a range of measurement techniques. The results are then compared with those derived from other published reports of precessing and flapping flows.

1.2. *Characteristics of precessing flows*

An important dimensionless parameter used to characterize precessing and flapping flows is the Strouhal number, a dimensionless frequency. The parameter has com-

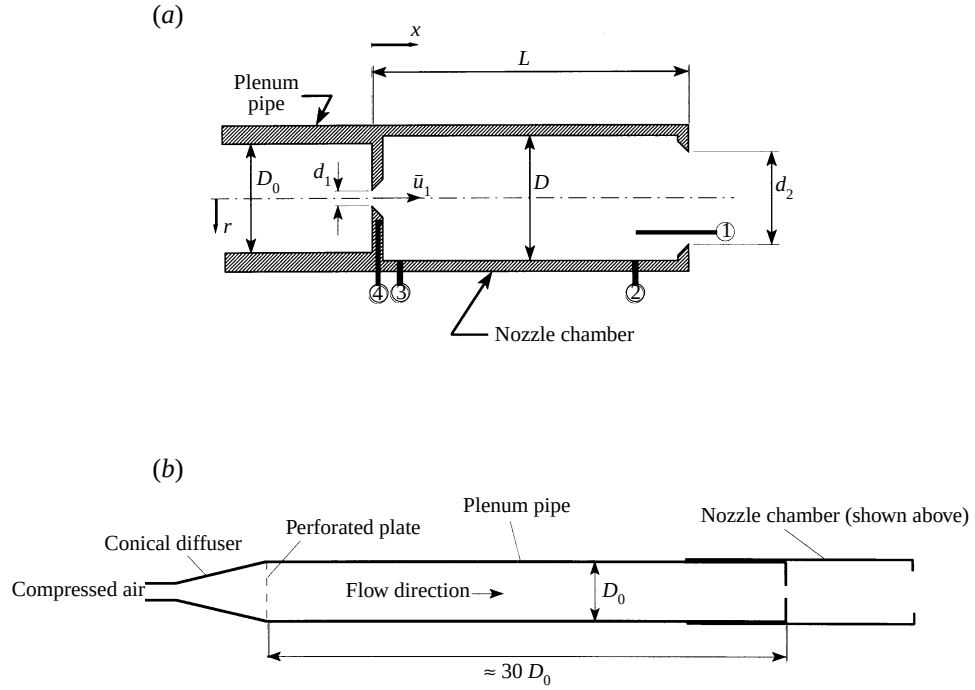

FIGURE 1. Schematic diagrams of the precessing jet nozzle and supply pipes. The notation and the locations of the probes for the measurement of fluctuating resssure are shown in the enlarged view (*b*) of the nozzle.

monly been applied to the vortical motions in the shear layer, but can also be used to characterize the larger scale flapping and precessing motions described above. Nathan & Luxton (1992*a*, *b*) compared several definitions of the Strouhal number of precession, St_p, to determine which best collapses the data over a wide range of flows and dimensions for the fluidic nozzle shown in figure 1(*a*). They found from measurements in both air and water that $St_{p,h} = f_p h/\overline{u_1} \approx 5 \times 10^{-3}$, where f_p is the characteristic frequency of the precession, $h = (D - d_1)/2$ is the step height of the expansion (see figure 1*a*) and $\overline{u_1}$ is the bulk mean velocity through the sudden expansion. While they found that the step height is a better characteristic dimension than the diameter at the inlet to the chamber, d_1, the Strouhal number based on the inlet diameter is the parameter most commonly documented in other studies, particularly for shear-generated structures. For the same data, but based on the inlet diameter, they derived $St_{p,d_1} = f_p d_1/\overline{u_1} \approx 2 \times 10^{-3}$. More recently, Hill *et al.* (1995) have examined the flow through a large sudden expansion into a very long downstream duct in apparatus which is accurately axisymmetric. They derived a Strouhal number which describes the precession based on the momentum, M, of the flow through the upstream orifice, d_1, and the diameter of the nozzle chamber, D, defined as:

$$St_{p,D} = \frac{f_p D^2}{(M/\rho)^{1/2}} \approx 0.08.$$

Hill *et al.* (1995) showed that in a long duct $St_{p,D}$ provides a better dimensionless description of the precession frequency for a wider range of expansion ratios than does $St_{p,h}$.

While the nozzle configuration under investigation (figure 1*a*) produces a precessing

flow instability, Nathan & Luxton (1992*a*, *b*) noted that the flow within it is generally bi-stable. Hill *et al.* (1992) characterized the two modes and described the dominant 'precessing jet' (PJ) flow mode, which is instantaneously highly asymmetric, and the less prevalent 'axial jet' (AJ) flow mode which briefly interrupts the PJ mode at irregular intervals. The characteristic features of both modes are investigated here in more detail using whole field visualization techniques and measurements of fluctuating pressure. The relative time spent in each mode is also quantified.

2. Experimental details

The flow within the nozzle has been investigated using whole-field flow visualization to characterize the broad features of the flow, surface flow visualization to quantify axial distances to lines of flow bifurcation, and simultaneous time-resolved pressure measurements at multiple points on the inner surface and within the flow inside the chamber to resolve flow modes and phase relationships. The configuration of the nozzle, relevant notation and the location of the wall-mounted and total pressure tappings are shown in figure 1(*a*). Two nozzles of the same general configuration have been used in the investigation. The larger Perspex nozzle, used for the investigations in air, has a chamber with a nominal internal diameter $D = 90$ mm. Detailed measurement has shown the chamber to be slightly ellipsoidal with the major and minor axes differing by 0.44% relative to a mean diameter of $D = 90.7$ mm. The inlet orifice, with a diameter $d_1 = 14.10$ mm was measured to be concentric to the chamber to within 0.3 mm. The chamber has an exit diameter $d_2 = 80$ mm and a length $L = 248$ mm. The axes of the nozzle chamber and the supply pipe were aligned to within 1 mm (radial direction) in 200 mm (axial direction). The smaller, accurately machined and polished acrylic nozzle used for the flow visualization in water, has a chamber diameter $D = 44$ mm, length $L = 114$ mm, inlet diameter $d_1 = 7.3$ mm, and exit diameter $d_2 = 35$ mm.

The Reynolds number used to describe the flow is based on conditions through the upstream orifice, d_1, i.e.

$$Re_1 = \frac{\rho \overline{u_1} d_1}{\mu},$$

where ρ is the density, μ is the dynamic viscosity and $\overline{u_1}$ is the bulk mean velocity entering the chamber through the orifice. The effect of Reynolds number has been investigated via the pressure measurements, from which it is determined that for the present geometry the precessing flow mode dominates when the inlet jet is fully turbulent. For all the flow visualization experiments $Re_1 \geqslant 15\,000$.

2.1. *Upstream and inlet flow conditions*

Figure 1(*b*) shows the layout of the upstream plenum pipe and diffuser used to supply flow to the nozzle. Considerable care has been taken to ensure that they provide an inlet flow to the nozzle chamber which is both unbiased and well defined. This ensures that the instability found to occur within the chamber cannot be attributed to rig-specific asymmetries or bias embedded within the upstream flow. The length of the plenum pipe is more than 30 times its diameter, D_0, to ensure that the flow presented to the inlet of the chamber is symmetrical and closely approaches fully developed turbulent pipe flow. At the inlet to the plenum pipe is a high-blockage perforated plate fed by an in-line conical diffuser with an included angle of 15°. The contraction ratio at the inlet to the nozzle chamber has an area ratio of 32. In summary the

overall arrangement has been carefully designed to provide an accurately symmetrical flow at the inlet to the nozzle chamber.

Flow symmetry in the plenum pipe has been checked by measuring mean axial velocity and turbulence profiles along fixed radii six pipe diameters ($6 \times D_0$) upstream from the inlet to the nozzle chamber. The data from a 5 μm tungsten hot-wire anemometer with a 1 mm active length was collected, unfiltered, at 1000 samples per second with 12 bit resolution and the frequency response of the anemometer was optimized to be flat to better than 3 kHz. At each measurement position, 15 360 samples were collected. The symmetry of the flow is evident from figure 2. In this figure, the data from each of the two orthogonal radial directions are reflected about the centreline and plotted on the same graph to provide a rigorous check of symmetry. Both the mean (figure 2*a*) and the turbulence (figure 2*b*) profiles for three values of pipe Reynolds number are closely symmetrical and show no consistent bias.

To check that the flow entering the nozzle chamber is also unbiased, velocity profiles of that jet issuing into free air (i.e. with the nozzle chamber removed) have been measured, using the same anemometer system, at $x/d_1 = 5$ for (interchangeable) orifice plates of four different diameters. The mean velocity profiles are shown in figure 3(*a*) and the turbulence profiles in figure 3(*b*). It can be seen that these profiles are also symmetrical and display good similarity.

Thus from the pipe flow and the free jet measurements it can be concluded that the precessing flow described later is not an artifact of the upstream conditions.

It is worth noting at this point that precession has also been observed in configurations for which the jet is introduced into the chamber through either a smooth contraction or through a long straight pipe of diameter smaller than that of the chamber. The smooth contraction generates a profile approaching the classic 'top hat' while the inlet velocity profile at the end of the straight pipe is that for fully developed pipe flow (Nathan 1988). For the present orifice plate the turbulence intensity in the above free jet experiments is high, peaking at about 65% in the middle of the shear layer. For the pipe flow the intensity is moderate, and for the smooth contraction the intensity is low. Hence we conclude further that the precessing phenomenon does not require unique or specific inlet flow conditions.

2.2. *Water flow visualization*

For the water flow visualization experiments the acrylic nozzle of internal diameter $D = 44$ mm discharges vertically upwards, to avoid trapping air in the nozzle chamber, into a transparent acrylic tank. The upstream supply pipe has a development length in excess of twenty diameters which follows an in-line pipe, a junction and another thirty diameters of straight pipe. This has been found to be more than sufficient to ensure that no asymmetry exists in the flow at the first orifice. Visualization is achieved by seeding the flow with small air bubbles, introduced well upstream from the nozzle. A broad, 30 mm thick, sheet of white light is directed through the axis of the nozzle. The images of the flow are recorded with a standard PAL video camera at 25 f.p.s. and with a 35 mm film camera at a range of shutter speeds. Both cameras are mounted perpendicularly to the plane of the light sheet. Other visualization techniques, using both neutral-density polystyrene beads and dye, have also been investigated. The character of the flow revealed by these techniques is indistinguishable from that revealed by the bubbles. Since the air bubble technique was found to provide the best image clarity, it is these images which are presented here.

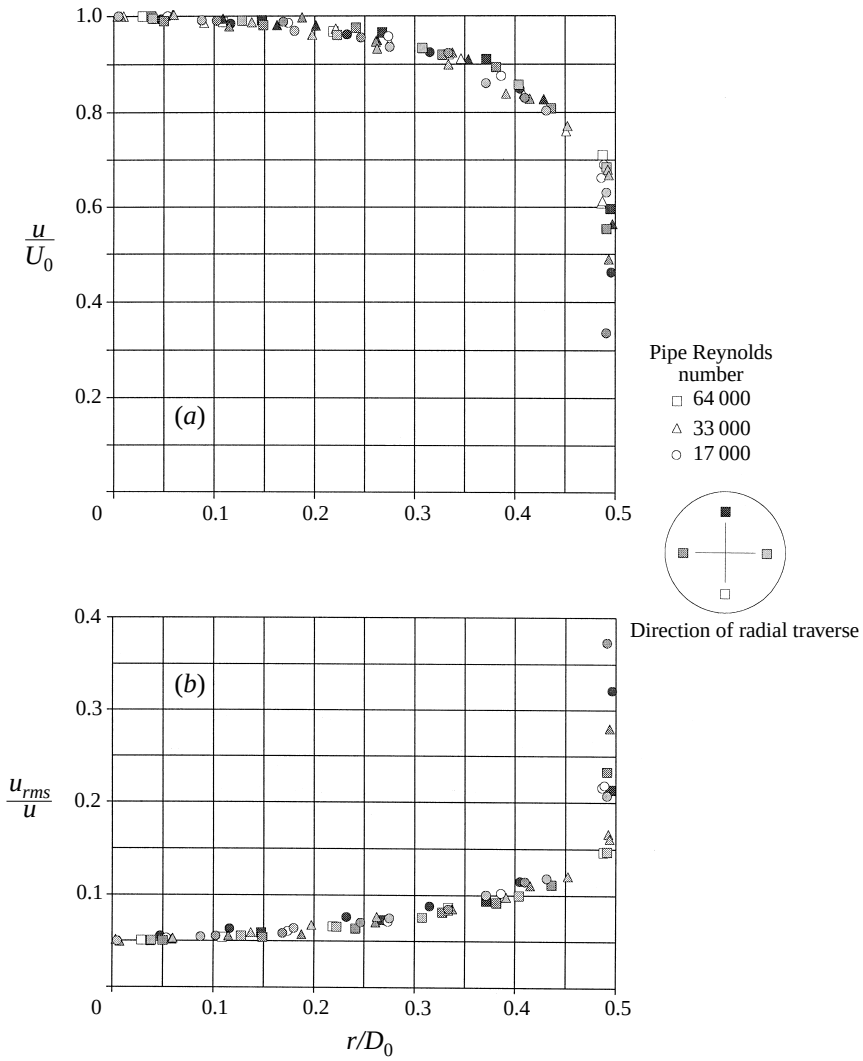

FIGURE 2. (*a*) Mean velocity and (*b*) turbulence intensity profiles in the plenum pipe measured six pipe diameters upstream from the nozzle inlet. The profiles are plotted from the centreline to the wall. The grey scale indicates the traverse orientation and the symbol shapes indicate each of three Reynolds numbers shown in the key.

2.3. *Wall and total pressure measurements*

Figure 1(*a*) shows both the coordinate system and the location of the three pressure tappings mounted on the inside surface of the chamber wall within the nozzle. Tapping 4 is located on the face of the sudden expansion as close to the nozzle axis as possible whilst ensuring it is clear of the bevel at the orifice, i.e. at $r/D = 0.21$, where r is the radial distance from the nozzle centreline. Simultaneous measurement of the wall pressure at location 3 and the face pressure at location 4 provides a good indication of the instantaneous radial pressure differential at the upstream end of the nozzle chamber. Pressure tapping 2 is mounted at $x/L = 0.89$, a position found from the surface flow visualization patterns to be downstream from the station at which the precessing jet reattaches to the surface. A total pressure probe at location

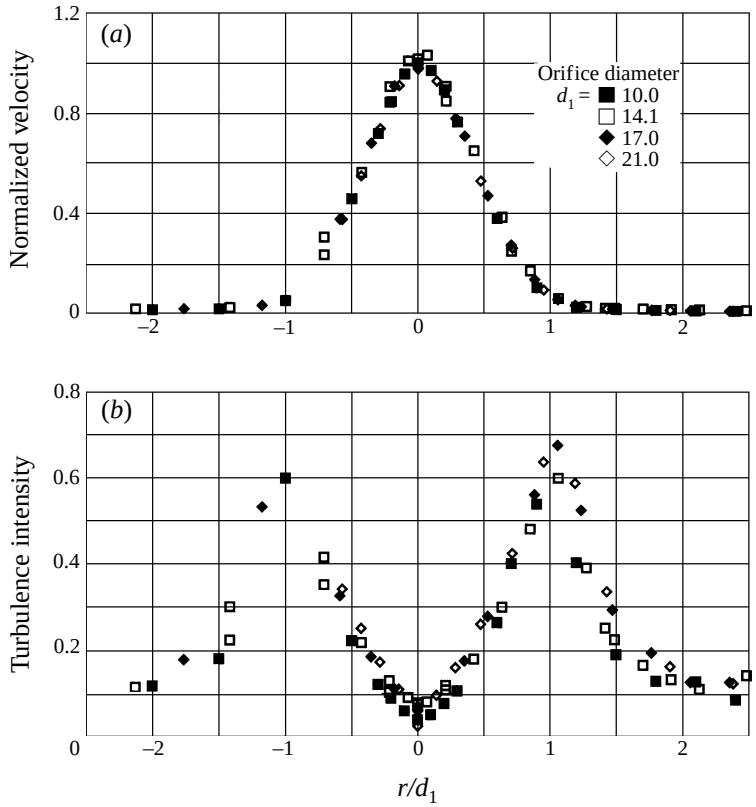

FIGURE 3. (*a*) Mean velocity and (*b*) turbulence intensity profiles of a free jet issuing through the throat, d_1, with the nozzle chamber removed. The measurements are at $x/d = 5$ for four different orifice diameters each with $Re_1 \approx 77\,000$.

1 is positioned with its tip at the same axial location as tapping 2. It is at a radial position, $r/D = 0.31$, which is near to the wall, and points upstream. Relative to ambient this probe registers a positive pressure when the jet is directed at it and a negative pressure in the presence of reverse flow.

The pressures at tappings 1–4 are measured relative to ambient using differential pressure transducers with a nominal frequency response of 1000 Hz. The length of the 1.3 mm diameter connecting hoses are less than 150 mm, which was found by Hill (1998) to avoid resonance and to attenuate frequencies of greater than 200 Hz. The signals from the four transducers are logged simultaneously on a personal computer at a rate of 500 Hz. Thus the response of the measurements is appropriate for resolving the typical precession frequency of 10 Hz.

2.4. *Surface flow visualization*

An impression of surface streak lines has been obtained by discharging air through a horizontally mounted acrylic nozzle, of internal diameter $D = 90.7$ mm, into ambient air. This diameter was selected to be as large as possible while remaining within the rated flow capacity of the air compressor/receiver system for the half-hour period required to dry a china clay mixture on the surface. The well known china-clay and oil-droplet techniques (Bradshaw 1970) have been combined to produce a relatively glutinous mixture of white china clay and oil of winter-green which 'holds up' on

vertical parts of the surface. The mixture is sprayed on a mat-black surface and the oil is evaporated while exposed to the flow to obtain a permanent record of the flow patterns over the inside surface of the nozzle, albeit a composite which is formed slowly during many cycles of precession (figure 16). To simplify the examination of the patterns so formed, a thin sheet of metal shim is rolled to form an inner skin which springs back hard against the chamber wall. The shim can be removed and unrolled for examination (figure 17), and the nozzle can be dis-assembled to reveal the pattern which is also formed on the face of the sudden expansion.

The liquid film forms into droplets which align themselves with the resultant of the shear and the gravity forces. The influence of gravity is greatest on those parts of the surface which are most nearly vertical but is found to be insignificant for Reynolds numbers greater than 10^5. This Reynolds number criterion sets the minimum flow rate for the surface flow visualization experiments. The glutinous consistency effectively filters out 'high'-frequency fluctuations. Observation indicates that the droplets formed in the mixture exhibit at best only a secondary response to fluctuations at the precession frequency, which in the present experiments is of the order of 10 Hz, and their gross motion records a time-smoothed path. Despite its limitations, this technique in association with the other forms of visualization and quantitative data, has proved to be extremely valuable in providing quantitative information on the position of surface reattachments and separations and in assisting in the interpretation of important features of the flow.

3. Results

3.1. *Flow visualization*

An image of the pathlines obtained from the water visualization technique while the flow is in the PJ mode is shown in figure 4. This figure also shows a schematic interpretation of the image developed from detailed observation of the video recording of the flow. The image captures the flow during that part of the cycle in which the plane of the reattaching jet is in the plane of the light sheet. The dominant features of the instantaneous flow within the chamber are labelled in figure 4 and are:

- a continuously unstable *reattaching jet* flow which is instantaneously asymmetric;
- a region of *recirculating fluid* which is located diametrically opposite the instantaneous location of the jet;
- a region of *swirling fluid* located in the most upstream part of the chamber;
- an *exiting jet* which is deflected across the axis of the chamber at a large angle;

Note that the entire flow field precesses (i.e. rotates azimuthally) about the geometric axis of the nozzle in a continuously unstable manner (see also Nathan & Luxton 1997).

Figure 4 suggests that the axial position at which the *reattaching jet* flow meets the surface is about halfway along the chamber and that the azimuthal position from which the jet leaves the chamber is approximately the same as that of the reattachment. The *exiting jet* is then deflected across the nozzle axis. Observation of a long sequence of video images indicates that the exit angle varies from cycle to cycle within the range of about 30°–70° relative to the nozzle axis. Other techniques have demonstrated that the exiting jet does not occupy the whole of the exit plane (Hill 1998 and Nathan & Luxton 1992*b*).

The *recirculated fluid* (figure 4) clearly contains fluid which originated from the jet, since only jet fluid is marked with the tracer. However other observations of a dye trace placed slightly outside the nozzle chamber show that ambient fluid is also drawn

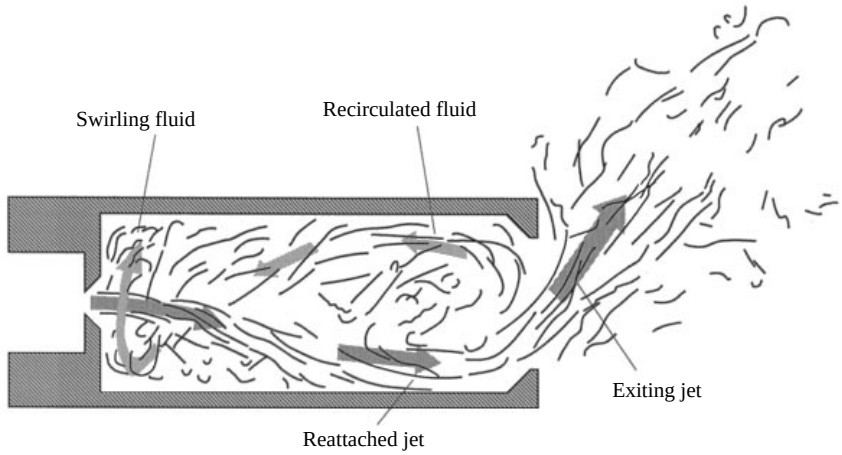

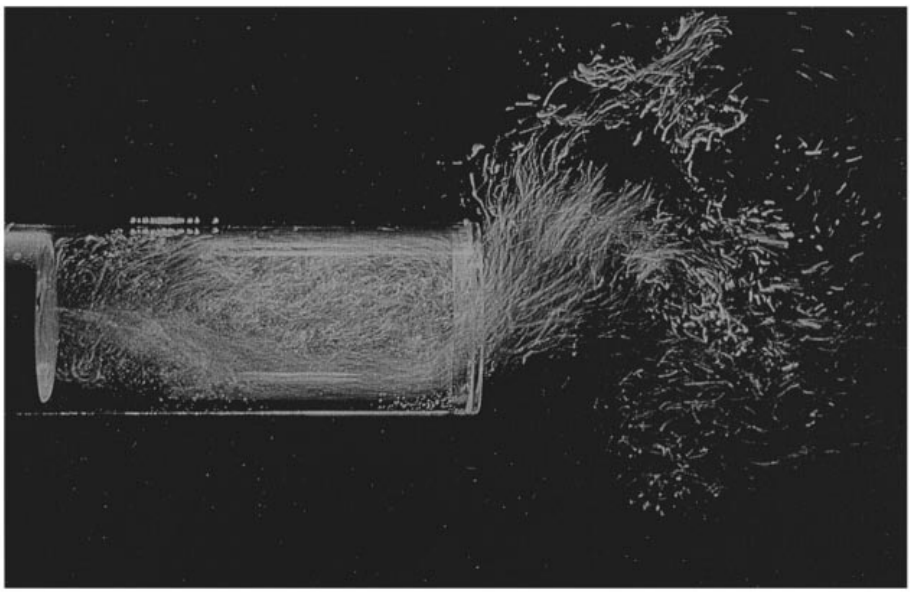

FIGURE 4. A light sheet image, obtained using the water flow visualization technique described in § 3.1, and a schematic interpretation of the instantaneous pathlines of the flow in the precessing jet (PJ) mode. Note that this entire flow field precesses about the nozzle axis. $Re_1 = 15\,000$, $D = 44$ mm, $L = 114$ mm, $d_1 = 7.3$ mm, $d_2 = 35$ mm.

into this region of recirculating fluid (Nathan 1988 and Nathan & Luxton 1992*a*). That result also indicates that the jet which leaves the chamber does not occupy the whole of the exit plane.

The region of *swirling fluid* in the most upstream part of the chamber is also evident in figure 4. Direct visual observation suggests that this motion is quite vigorous. Figure 4 shows that the axial extent of the swirling region is approximately $1/6 < x/L < 1/4$ and that the swirling flow is fed by the recirculated fluid.

The less dominant of the two flow bi-stable modes, the axial jet (AJ) mode, has also been visualized. Figure 5 shows the corresponding image and interpretation of

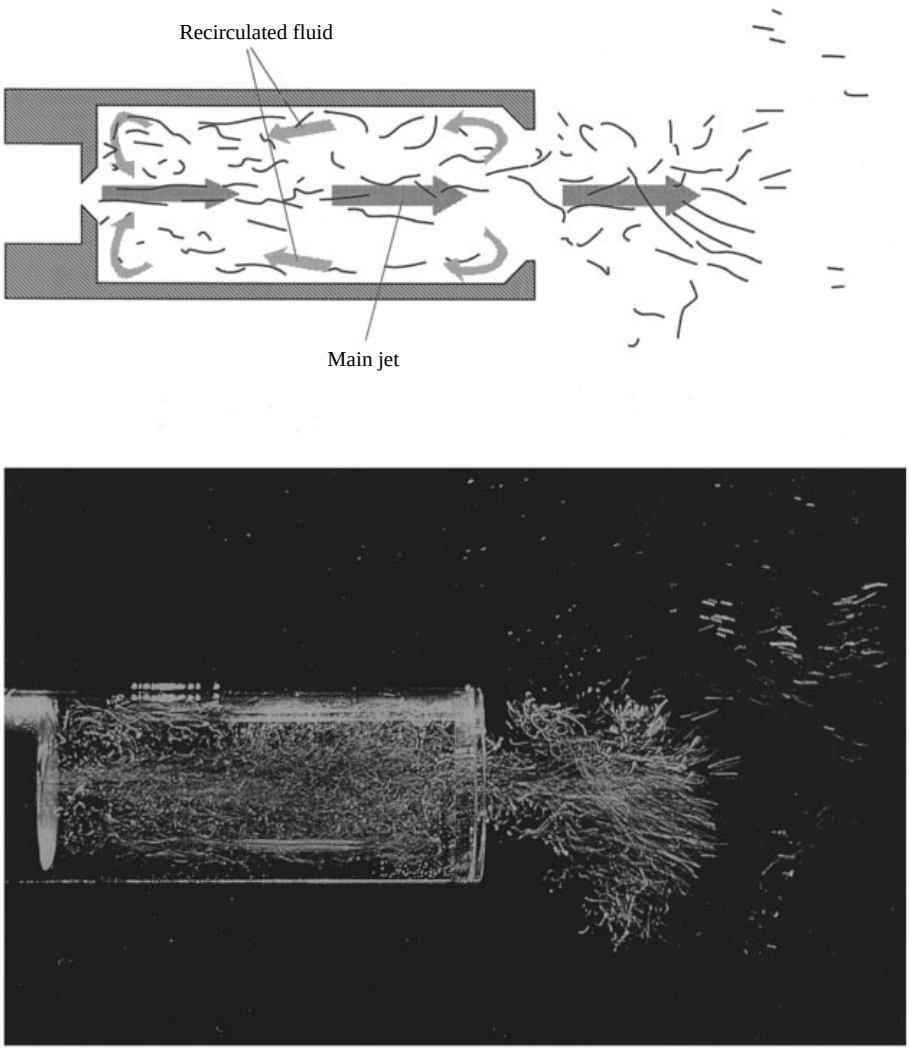

FIGURE 5. A light sheet image and schematic interpretation of the instantaneous pathlines of the flow in the axial jet (AJ) mode. (Conditions as specified for figure 4.)

the pathlines of that flow mode. Note that figures 4 and 5 were observed at different instants in identical geometric configurations with the same operating conditions. The AJ flow does not display the high degree of asymmetry found in the PJ mode and does not reattach to the wall within the nozzle chamber. However the jet does interact with the 'lip' at the exit plane resulting in flow structures of a larger scale than would exist if the nozzle chamber were to be removed (Nathan 1988).

Long-exposure photographs of the two flow modes were obtained by selecting a shutter speed corresponding to the time required for several cycles of precession (figures 6 and 7). These long-exposure streak images suggest that both flow modes are, on average, axisymmetric. However the jet produced by the PJ flow spreads much more rapidly than that of the AJ mode, indicating a correspondingly larger scale of mixing.

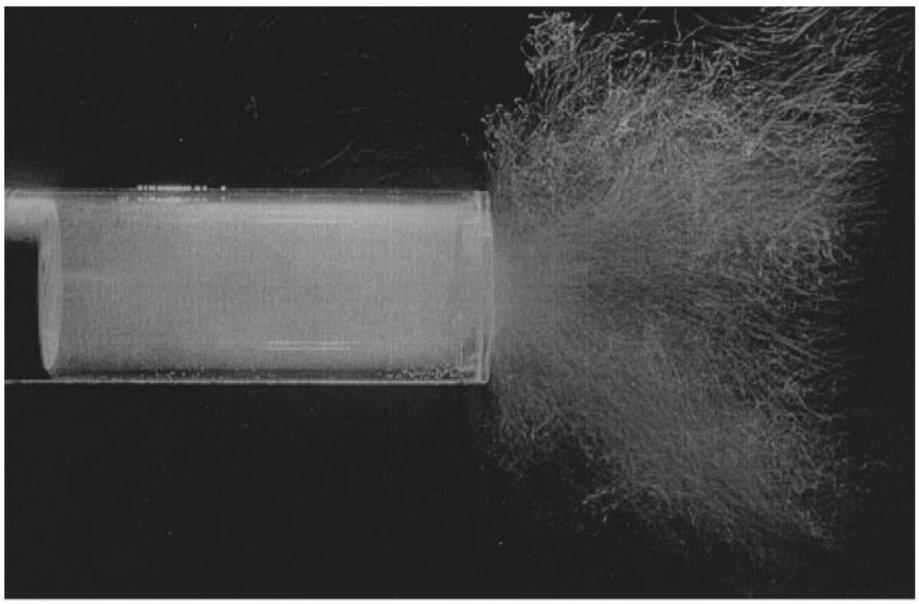

FIGURE 6. Long-time exposure photographs of the flow through the nozzle with the flow in the PJ mode. (Conditions as specified for figure 4.)

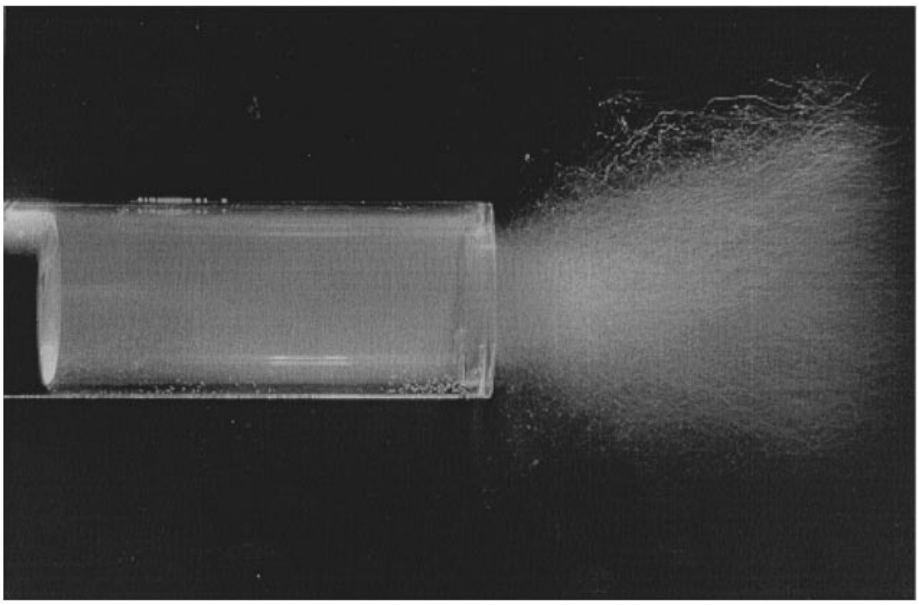

FIGURE 7. Long-time exposure photograph of the flow through the nozzle with the flow in the axial jet (AJ) mode. (Conditions as specified for figure 4.)

The full-field flow visualizations have provided a clear demonstration that two distinct and bi-stable flow modes are generated within the present cylindrical nozzle chamber when the inlet jet is turbulent (here $Re_1 = 15\,000$). In the PJ mode which is visually observed to dominate, the jet reattaches asymmetrically to the chamber wall and the entire flow field precesses within the chamber. The dominant features

of this flow have been identified. In the other flow mode, termed the AJ mode, the jet interacts with the exit lip but does not truly reattach within the chamber. The resulting jet which emerges from the nozzle chamber spreads much more rapidly in the PJ mode than in the AJ mode.

3.2. *Fluctuating pressure measurements*

Quantitative data relating to each of the two flow modes has been obtained by measuring the fluctuating pressure field simultaneously at four points within the nozzle chamber. Figure 1(*a*) shows the location of the three pressure tappings mounted in the chamber wall and of the total pressure probe, which were all measured simultaneously relative to ambient. The total pressure probe 1 is positioned off-axis to detect quantitatively the gross features observed in the visualization and so to enable the discrimination between the two flow modes. The axial position of the total pressure probe 1 is downstream from the plane of the reattachment observed for the PJ mode, but for the AJ mode, in which the jet does not reattach to the chamber wall, the probe is within the region of reverse flow (figure 5). Its radial position is chosen to coincide roughly with the centre of the eccentric *reattached jet* of the PJ mode (figure 4). The off-axis location of total pressure probe 1 means that, when the flow is in the PJ mode, it will be subjected to a strong pressure fluctuation each time the jet sweeps past it but when the flow is in the AJ mode those quasi-periodic, low-frequency pulsations will not be present. Furthermore the tip of the probe, when the flow is in the AJ mode, falls within the annular reverse flow region around the jet and so will record a negative pressure relative to ambient. The static pressure tappings are positioned to allow measurement of the fluctuating pressure gradients in the axial and radial directions.

A representative segment of the time history of the pressure fluctuations is shown on three progressively finer time scales, all referenced to the same absolute time base, in figures 8 to 11. It is evident from figure 8 ($0 < t < 480$ s) that a strongly fluctuating signal is present for most of the time in the traces of both the total pressure (1) and wall pressure (3) probes, punctuated with short bursts during which the pressure in both traces is markedly reduced. The subsequent plots demonstrate that the dominant signal is caused by the PJ mode and that the distinct drop in the upstream wall pressure, corresponding well with the cessation of the pressure cycles recorded by the total pressure probe, is produced by the AJ mode. The contrasting features in the details of the PJ and AJ flow modes are clearly evident in figures 10 and 11 respectively. The cyclic nature of the oscillation produced when the jet sweeps past the total pressure probe in the PJ mode is apparent in figure 10 ($228.4 < t < 228.8$ s). By contrast these pulsations are absent in figure 11 ($224.6 < t < 225.0$ s). At the same time there is a distinct difference in the wall pressure at the upstream end of the chamber, position 3, in the two modes – being more negative in the AJ mode. This is also evident in figure 9 which shows a 10 s time segment, during which the flow is predominantly in the PJ mode but where the flow switches for about 3 s into the AJ mode.

The significant differential pressure between positions 3 and 4 (figure 10) that is present during the PJ mode is evidence of a strong radial pressure gradient at the upstream end of the chamber. This differential is much smaller in the AJ mode. The direction of the pressure gradient in the PJ mode is consistent with the presence of a swirling flow, as observed in the whole-field visualization and as can be deduced from the surface flow visualization described later. The presence of a general reverse flow in both modes is evidenced by the axial pressure gradient which shows that the

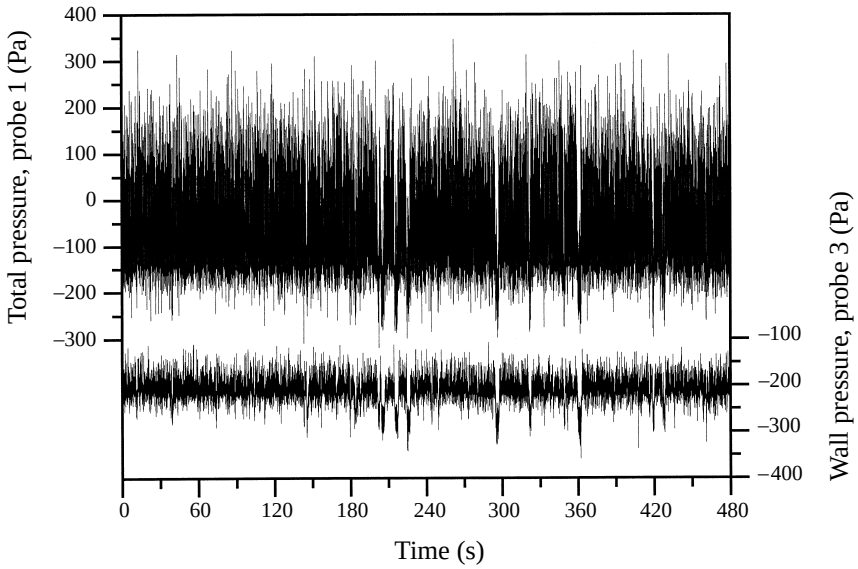

FIGURE 8. Representative segments from a time record of a total pressure (position 1) and wall pressure (position 3) traces measured in air at locations shown in figure 1. The precessing jet (PJ) mode dominates, interspersed by short bursts of axial jet (AJ) mode. The AJ mode is evidenced by a lower pressure in both signals. Conditions: $Re_1 = 76\,700$, $D = 90.7$ mm $d_1 = 14.1$ mm, $d_2 = 80$ mm, $L = 248$ mm.

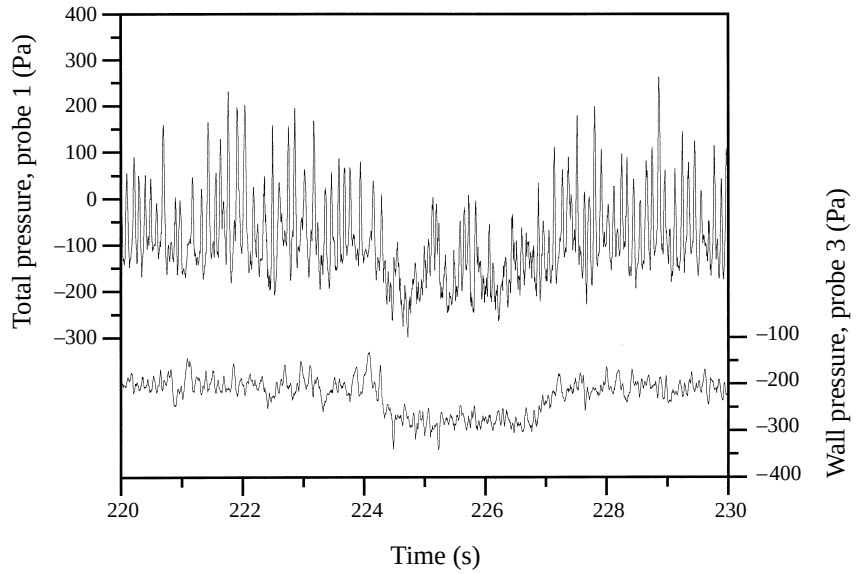

FIGURE 9. A short segment from the temporal pressure traces shown in figure 8. More details of the differences between the total and a wall pressure traces which occur in the precessing jet and axial jet flow modes can be seen. Conditions as specified for figure 8.

magnitude of the wall pressure at the inlet end of the nozzle chamber is generally more negative than that nearer to the exit (position 2). However, differences in the nature of the reverse flow in each mode (in addition to the upstream radial pressure gradient already described) are also apparent in the pressure traces, and these are

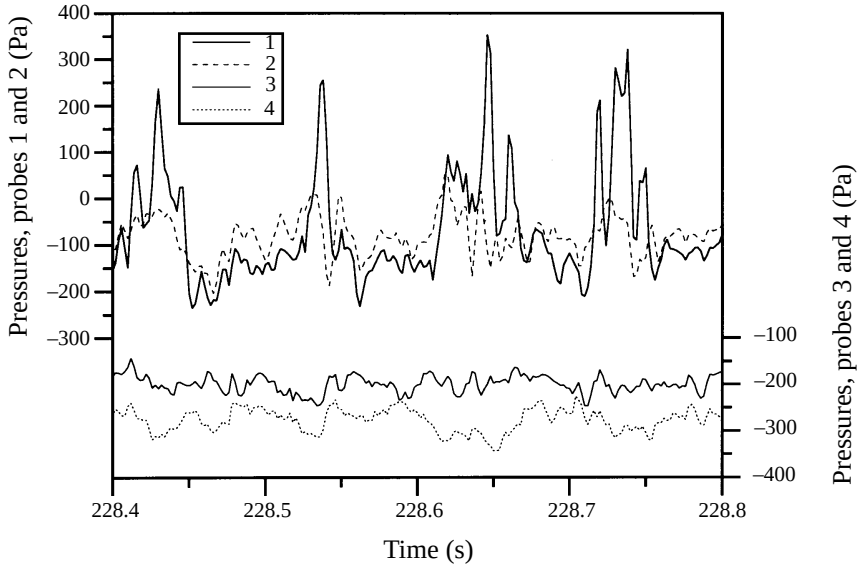

FIGURE 10. A magnified time base showing, in detail, the pressure fluctuations during several cycles of precession. The pressure is measured at all four locations shown in figure 1(*b*). Conditions as specified for figure 8.

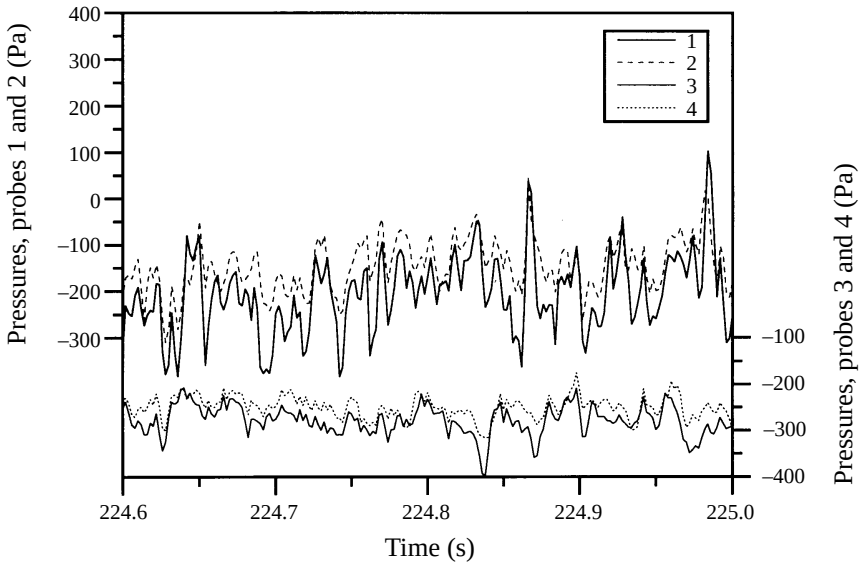

FIGURE 11. A magnified time base showing the axial jet flow mode in detail using all four pressure measurement points indicated in figure 1(*b*). Conditions as specified for figure 8.

consistent with the differences evident in the flow visualizations. The wall pressure at the outlet end of the chamber (position 2) is more negative in the AJ mode than in the PJ mode. The smaller-scale fluctuations in the pressure traces are also different in the chamber.

In the PJ flow mode a negative correlation exists between the cyclical pressure fluctuations on the upstream face of the chamber at position 4, and the total pressure

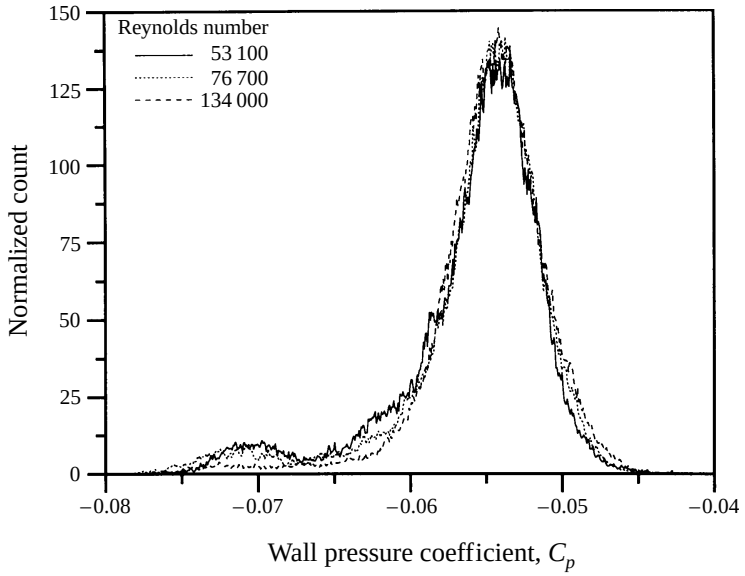

FIGURE 12. The normalized probability density functions (p.d.f.) of wall pressure at position 3 used to determine the amount of time spent in each flow mode. The working fluid is air and the nozzle dimensions are as specified for figure 8.

at position 1 downstream from the reattachment. This indicates that the swirling flow is not uniform in the circumferential direction, and is consistent with the observation that the swirling flow is fed by fluid from the recirculating region. It is postulated that the pressure at position 4 is higher due to the recirculated fluid being carried to the back of the chamber, where it is caused by the wall blockage to slew to one side and thus to feed the swirling flow.

The observation that different average wall pressures at position 3 are associated with each of the two modes provides a means for discriminating between the modes, and hence a means by which to quantify the relative time spent in each mode. The signal is low-pass filtered at half the frequency of precession and the normalized probability density function (p.d.f.) of that pressure is plotted in figure 12, so that $\int_{-\infty}^{+\infty} N \, \mathrm{d}C_p = 1$, where N is the normalized number of times at which a given pressure is recorded within the measurement period. The filter eliminates fluctuations in pressure caused by each cycle of precession but retains the longer-time-scale fluctuations caused by mode switching. Data are presented for three Reynolds numbers, normalized so that the pressure coefficient on the abscissa, C_p, is the wall pressure at position 3 normalized by $\rho\overline{u_1}^2/2$. A 'correction' (1.5% and 11% for the intermediate and high Reynolds number cases respectively) has been applied to the normalizing bulk mean velocity of two curves to obtain good collapse. This correction is merely to allow the same value of C_p to be used for the discrimination in each curve and does not influence the value which is calculated for the proportion of time spent in the PJ mode, $Prob(PJ)$. It is deduced that the correction is required because of compressibility effects (see discussion below).

The general shape of the p.d.f. is bi-modal with two (approximately Gaussian) peaks being superimposed. The right-hand peak, centred at $C_p \approx -0.054$, corresponds to the PJ mode, while the left-hand peak, centred at $C_p \approx -0.071$, corresponds to the AJ mode. In the present case a cut-off has been selected at $C_p = -0.067$, based

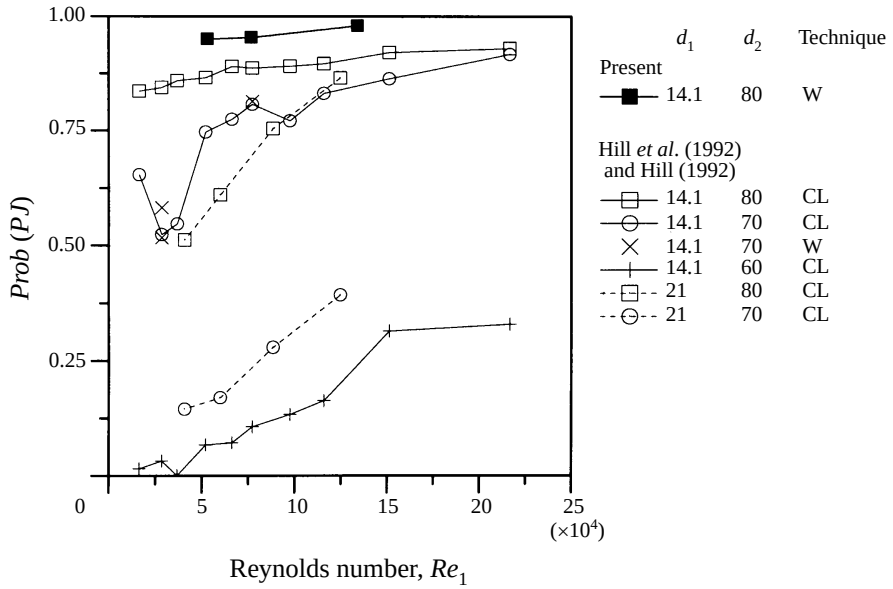

FIGURE 13. The proportion of time spent in the precessing jet flow mode, $Prob(PJ)$, as determined in the present study, compared with that of Hill (1992) and Hill *et al.* (1992) for a range of nozzle geometric configurations. The technique used to discriminate the modes is a p.d.f. of the pressure measurement at the wall, denoted W, or of the signal from a total pressure probe on the centreline, denoted CL. The nozzle dimensions are as specified for figure 8. The notation is given in figure 1(*b*).

(somewhat arbitrarily) on the lowest point in the saddle between the two peaks, to allow discrimination between the two modes. The areas under the right and left peaks then correspond approximately to the proportion of time that the flow spends in the PJ mode, denoted $Prob(PJ)$, and the AJ mode, $Prob(AJ)$, respectively. This leads to $Prob(PJ) = 0.950$ for $Re_1 = 53\,100$, $Prob(PJ) = 0.953$ for $Re_1 = 76\,700$ and $Prob(PJ) = 0.979$ for $Re_1 = 134\,000$, in agreement with the dominance of the PJ mode demonstrated from figure 8 and the increasing dominance of the PJ mode with Reynolds number.

The percentage of time spent in the PJ mode, $Prob(PJ)$, is plotted in figure 13 as a function of the inlet Reynolds number, Re_1. The data of Hill (1992) and Hill *et al.* (1992) also presented in this figure to provide a comparison with results from smaller data sets obtained in apparatus with different inlet flow conditions. Despite the differences in the detail of the results, as expected from the previous comments, the broad agreement between the two sets of data is clear evidence that similar gross features are present in the flows produced in the two sets of apparatus. It is evident that the stability of the PJ mode increases with Re_1 and that it dominates for the range of Reynolds numbers presented here ($Re_1 > 50\,000$). It is also evident that $Prob(PJ)$ is strongly dependent upon nozzle geometry, with an exit diameter of $d_2 = 80$ mm ($d_2/D = 0.89$) favouring precession more than $d_2 = 70$ mm ($d_2/D = 0.78$), and an inlet diameter of $d_1 = 14.1$ mm ($d_1/D = 0.16$) favouring precession more than $d_1 = 21$ mm ($d_1/D = 0.23$).

The frequency spectra of the pressure trace recorded by total pressure probe 1 are shown in figure 14 for the three Reynolds numbers. These spectra are averaged from 58 separate spectral records, each generated from blocks of 4096 independent samples. The low-frequency peak associated with the precession is clearly evident.

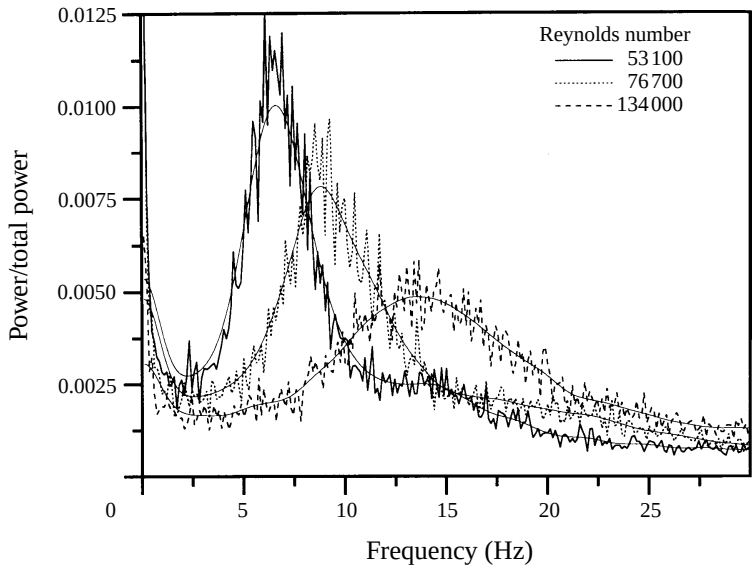

FIGURE 14. Frequency spectrum of the fluctuations from a total pressure probe (number 1) showing the dominant frequency of the precessing mode. Conditions as specified for figure 8.

Re_1	$St_{p,M}$	St_{p,d_1}	$St_{p,h}$
53 100	0.0726	0.00155	0.00422
76 700	0.0640	0.00137	0.00372
134 000	0.0786	0.00168	0.00457

TABLE 1. A comparison of the Strouhal numbers measured for the PJ mode as a function of the inlet Reynolds number. Nozzle dimensions are the same as those specified for the traces in figure 8.

The shape of the peak is not sharp, but broad, indicating that the frequency of the precession, while possessing a characteristic mean value, fluctuates significantly. Large cycle-to-cycle variations in the precessional flow are also evident by direct observation during the flow visualization experiments, and from the study of video recordings. The frequency spectra are also consistent with previous observations (Nathan 1988) and with the time record shown in figures 9 and 10. The Strouhal number associated with the peak frequency has been calculated based on the three definitions given earlier. The data are presented in table 1.

The Strouhal numbers measured in the present facility, which provides axisymmetric and well defined flow to the nozzle chamber, are compared with previous measurements in figure 15. A definition of Strouhal number based on inlet diameter, $St_{p,d}$, is used to enable direct transcription of the data from the literature. The data of Nathan (1988) were obtained from the frequency spectra as measured by a hot-wire anemometer located in a similar position to the total pressure probe used in the present investigation. Those measurements were conducted in the same nozzle chamber as that used for the present data but with slightly different inlet conditions. The length of the supply pipe immediately upstream from the nozzle chamber in the earlier study was only five pipe diameters (i.e. $5 \times D_0$) and no perforated plate was placed at the exit from the upstream diffuser (see figure 1*b* for reference). The

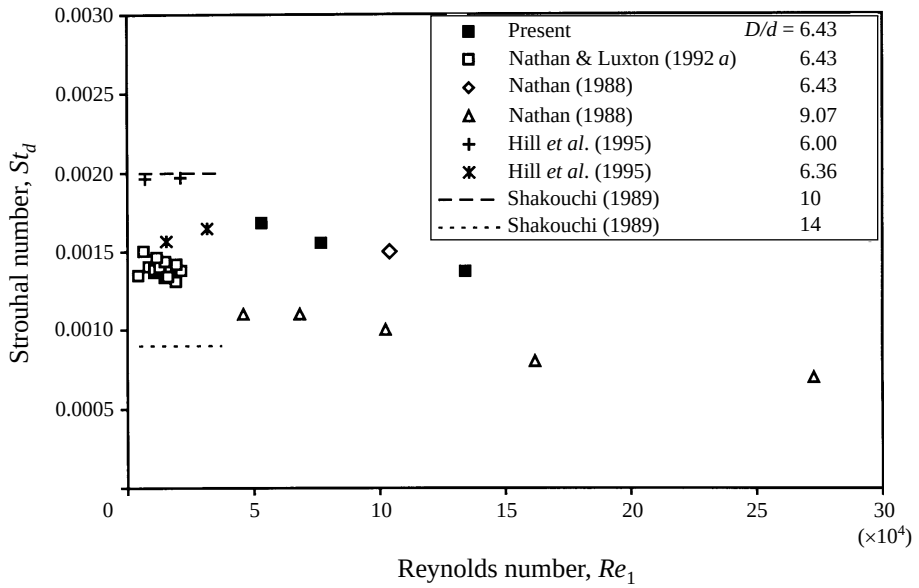

FIGURE 15. The Strouhal number of precession found from the present data compared with data from earlier investigations and with those by Shakouchi (1989) for flapping motions in a comparable two-dimensional configuration. Present nozzle geometry as specified for figure 8.

conditions did not produce fully developed pipe flow at the inlet to the chamber, although the mean flow was shown to be axisymmetric. The data of Nathan & Luxton (1992*a*) were obtained with water as the working fluid and employed a visual technique in which the number of cycles was counted manually over long periods and then averaged. The nozzle was the same as that used by Nathan (1988) with air as the working fluid. The data of Hill *et al.* (1995) were also obtained from the manual counting of precession cycles in flow through a sudden expansion, but this time into a long downstream duct instead of a nozzle chamber. A smooth contraction was used at the inlet to that pipe, with diametral contraction ratios of 5 and 10. The contraction, in turn, was downstream from a large plenum pipe with a length of ten pipe diameters (i.e. $10 \times D_0$). The working fluid was water and neutral-density polystyrene beads were used to image the flow. The data of Shakouchi (1989) were obtained in a planar facility which is otherwise broadly analogous to the present configuration. The peak frequency from a wall-mounted pressure tapping was measured and was found to coincide with a large-scale flapping oscillation within the chamber. The data presented here are the upper and lower bounds of Strouhal numbers found in this wide parametric investigation.

The data presented in figure 15 were obtained with three different experimental techniques and in four different facilities, three of which are cylindrical and produce a flow with a precessing motion while one is planar and produces a flow with a flapping motion. The figure contains both data collected from configurations with an orifice plate at the inlet and from configurations with a smooth contraction. It also contains data obtained with two different working fluids. All of the data in figure 15 were obtained with residual turbulence from the upstream pipe or duct flow entering the respective downstream chambers and the Reynolds numbers were all sufficiently high for the inlet jet to be turbulent. The good agreement between the wide range of data sets suggests that the underlying large-scale flow instability in each case is

closely related. That St_{p,d_1} is dependent upon the expansion ratio at the chamber inlet is clearly evident. The dependence of St_{p,d_1} upon the inlet Reynolds number is only observed in those configurations conducted in (compressible) air when that air is introduced into the chamber through an orifice plate, which necessarily produces a vena contracta. The dependence is not observed in the investigations conducted using water with either inlet condition despite the presence of a vena contracta for the orifice entry. The maximum Mach number of the inlet flow through the vena contracta for the present data has been estimated to be about 0.7. At this Mach number, compressibility effects can be expected to become significant and to influence the vena contracta. Thus it is suggested that compressibility effects are the probable cause of the Reynolds number dependence with air flowing through orifice plates. It should be noted that the data of Shakouchi (1989) show St_{f,d_1} to be independent of Re_1 when the Reynolds number is sufficiently large.

The fluctuating pressure measurements have provided quantitative measurement of the major features of the PJ and AJ flow modes. The low-frequency fluctuation found in the trace recorded by the off-axis total pressure probe is clearly evident in the PJ mode and absent in the AJ mode. The value of Strouhal number associated with these fluctuations as determined in the present study, $St_{p,d_1} \approx 0.0015$, agrees well with data obtained previously by a range of probe techniques in other facilities. It also agrees very well with that determined visually by counting the cycles of precession observed in the visualization experiments, so confirming that this Strouhal number is associated with the same large-scale motion of the jet. The radial pressure gradient measured at the upstream end of the chamber is found to be present in the PJ mode and absent in the AJ mode. These features have been used to discriminate between the two modes and so to quantify the proportion of time spent in each mode. For the range of geometries and conditions studied, the PJ mode is dominant.

3.3. *Surface flow visualization*

Surface flow visualization experiments have been conducted to provide a measurement of the axial positions of the dominant surface flow features present in the PJ mode. Related techniques have been shown by many others (e.g. Tobak & Peake, 1979 and Hunt *et al.* 1978) to be effective when investigating 'steady' flows around a body. Hornung & Perry (1984) have documented and defined the main classes of three-dimensional separated flow and their surface flow footprints. Their terminology is followed here and includes lines of 'open' or 'closed' 'bifurcation' which can be either positive (for reattaching flow) or 'negative' (for separating flow). An example of a line of positive bifurcation is the stagnation streamsurface on an infinite swept cylinder which divides along the stagnation line. An open bifurcation line occurs in three-dimensional flow and is discontinuous. An example is the separation which occurs near the leading edge of a body of revolution at high angles of attack. That separation does not extend around the entire circumference of the body, so it is 'open' (Wang 1974 and Tobak & Peake 1979). In the present case the reattachment of the jet in the PJ flow mode has been observed in the liquid flow visualization to be discontinuous around the inner circumference of the chamber wall (figure 4) and so is known to be in the nature of an open line of positive bifurcation. However, in contrast to the above example of the body at a high angle of attack, which is fixed in space and time, the present line of positive bifurcation can be deduced to move, that is to precess around the inside of the chamber.

It is apparent from the pressure measurements and from the whole-field visualization that each point on the surface is exposed to cyclical shear stresses when the

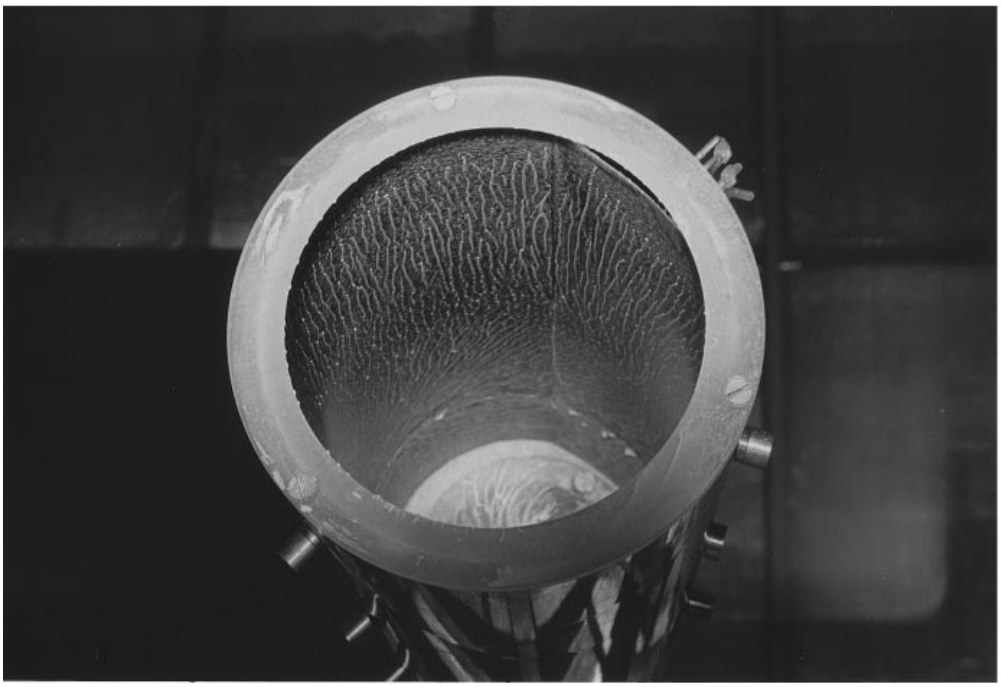

FIGURE 16. View through the nozzle exit into the nozzle chamber showing the china clay pattern formed on a removable thin metal shim attached to the inner wall.

flow is in the dominant PJ mode. An additional change to the surface shear stresses occurs intermittently for brief periods when the flow switches to the AJ mode. However the Reynolds number selected for the surface flow visualization experiments, $Re_1 \approx 10^5$, is high so that, from figure 13, $Prob(PJ)$ has been estimated to be 98%. The response time of the surface flow visualisation technique is, intentionally, very much slower than the characteristic frequency of precession in the PJ mode. Thus, rather than revealing the open bifurcation lines of the actual instantaneous footprint of the unsteady flow, the technique responds to the dominant surface flows in the cycle and reveals apparently closed lines as these features rotate around the chamber. Despite the absence of circumferential or temporal resolution of the flow footprints, the technique provides quantitative information about the mean axial positions of the dominant bifurcation lines.

The view into the nozzle chamber, showing the streak patterns on the inner surface, is shown in figure 16. Figure 17 shows the clay-covered shim after being removed and opened out flat to reveal the 'average' positions of the dominant surface flow patterns formed on the entire inside surface of the nozzle chamber. The principal features identified here, and supported with enlarged views (figures 18 to 21) and their respective interpretative sketches are:

- a *transverse* (*azimuthal*) *flow* (i.e. swirl) in the upstream section of the chamber;
- an *upstream negative bifurcation line* located approximately one-quarter of the chamber length from the inlet plane;
- a *positive bifurcation line* near to the middle of the chamber, and
- a *downstream negative bifurcation line* located immediately upstream from the exit plane.

The *transverse swirling* flow in the upstream part of the chamber can also be seen

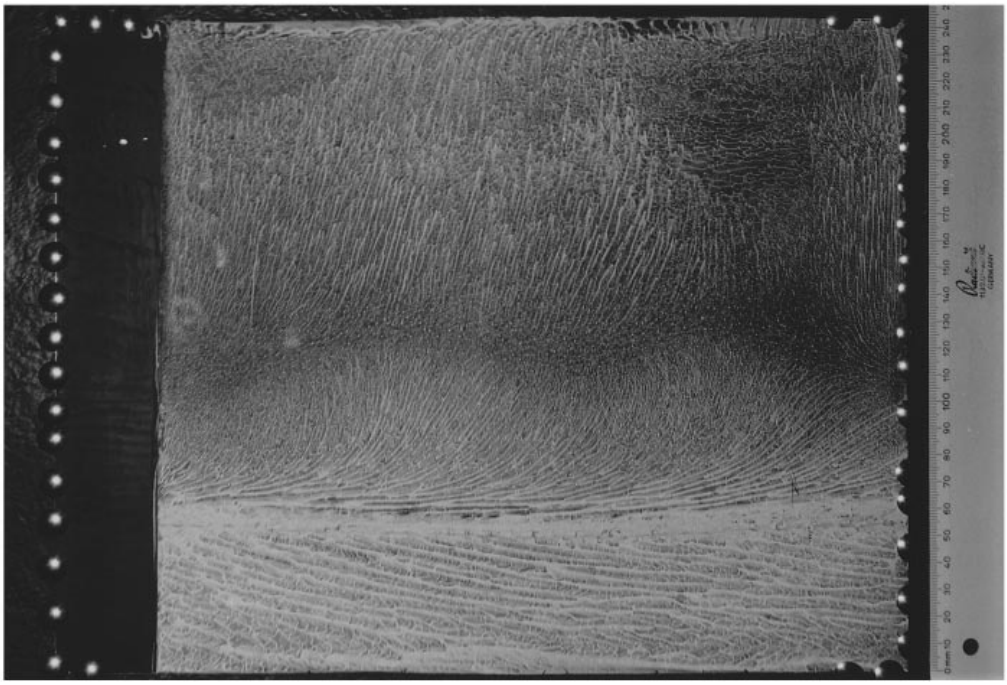

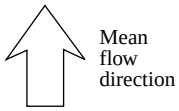

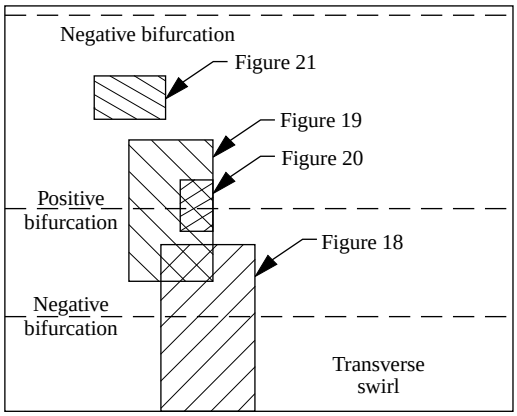

FIGURE 17. Global image of the streak patterns fromed on the inside surface of the chamber by the surface flow visualization technique after the metal shim has been removed and unrolled. The accompanying line diagram identified the major features evident in the patterns and locates the detailed enlargements shown in figures 18–21. $Re_1 \approx 28 \times 10^4$, $D = 90.7$ mm, $L = 245$ mm, $d_1 = 14.1$ mm, $d_2 = 80$ mm.

in figure 22 which shows the direction of the flow over the upstream orifice plate. These images are consistent with a flow whose dominant motion is an inwardly spiralling swirl, identified previously in the pressure measurements and in the whole-field visualization.

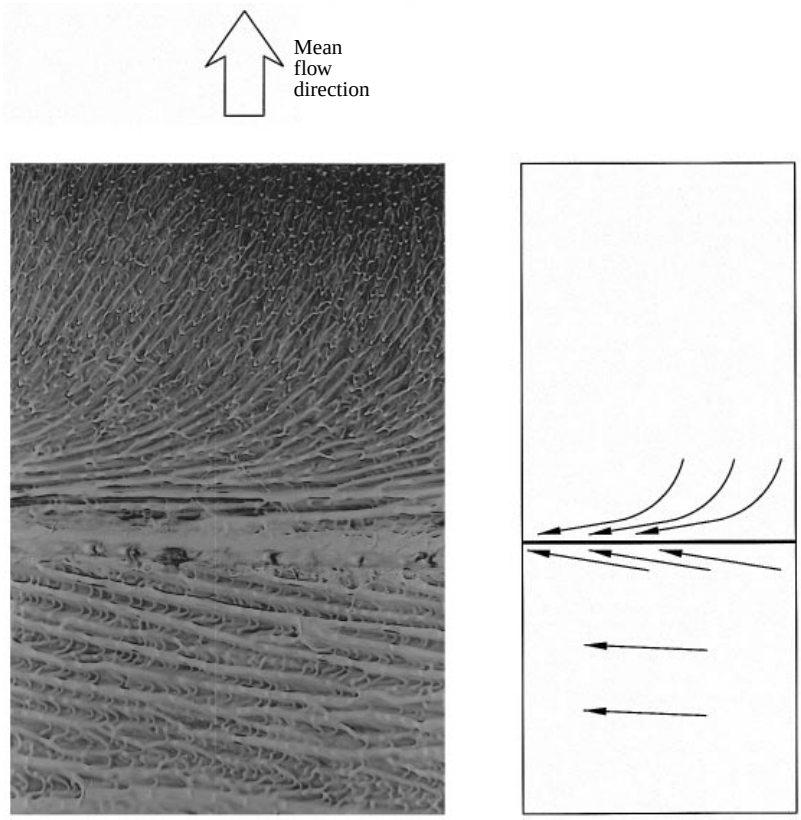

FIGURE 18. Enlargement of the surface flow image of the upstream negative bifurcation line. Note the strong azimuthal swirl evident in the pattern as the flow approaches the negative bifurcation. (Conditions as specified for figure 17.)

An enlarged view of the upstream *negative bifurcation* line is shown in figure 18, with an interpretative sketch of the dominant flow directions. The axial components of flow on both sides of the line are clearly toward the bifurcation line. The strong swirl on the upstream side is again evident.

Photographs identifying the line of *positive bifurcation* are shown with their interpretative sketches in figures 19 and 20. The axial direction of the dominant flow is clearly away from the line. The axial position of this line, near to the middle of the chamber, can be seen to correspond closely to the location of the reattachment observed in the whole-field images of the PJ mode (figure 4), which lends support to the proposed interpretation of the surface patterns. The dominant flow in the region upstream from the positive bifurcation can be seen to slew with an increasingly strong azimuthal component until it becomes tangential at the line of negative bifurcation. Whether the bifurcating flow is associated with the recirculated fluid, which originates from the interaction between the jet flow and the exit lip, or with the flow which moves upstream from under the reattaching jet ('the reverse flow foot') cannot be determined from this technique. However, careful observation of whole-field visualization suggests that the former flow is the stronger of the two and that the line of negative bifurcation is formed as the recirculated fluid swirls back on itself. The whole field visualisation also suggests that the upstream negative bifurcation line is about 180° out of phase with the positive bifurcation line.

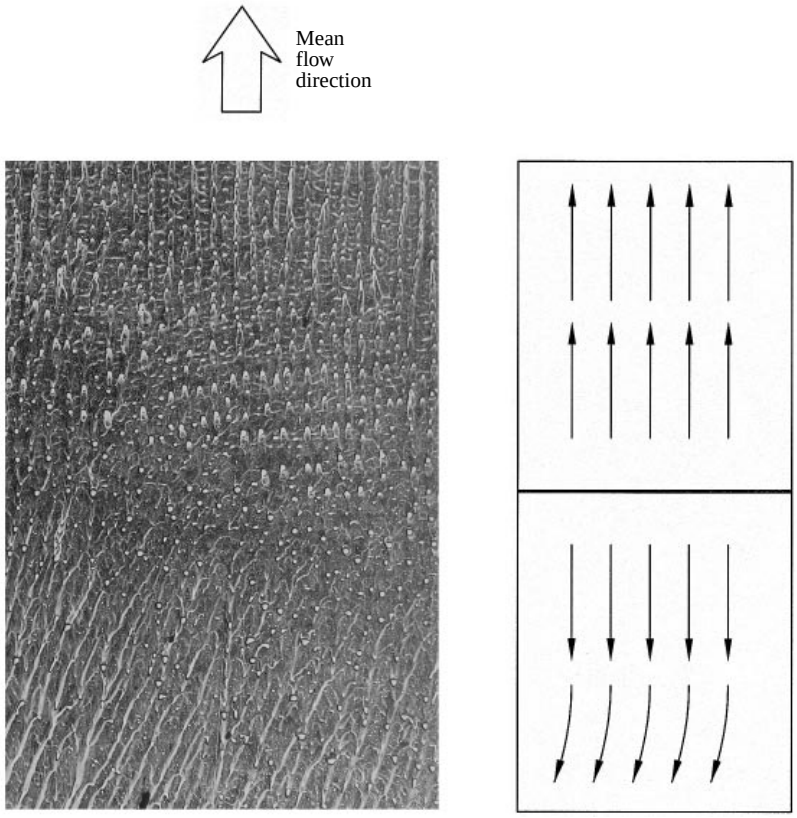

FIGURE 19. Enlargement of the flow patterns formed upstream and downstream from the positive bifurcation line. Note the differences in the character of the patterns upstream and downstream from the bifurcation. (Conditions as specified for figure 17.)

Close observation of the surface flow pattern in the region downstream from the line of positive bifurcation also indicates an intermittent flow (figure 21). The surface streaklines appear to exhibit both a primary response to the strong downstream flow produced by the reattached jet, and a secondary response to a weaker upstream flow which we deduce to be caused by the recirculated fluid passing over them as the reattachment point moves around the circumference. Thus the drops appear to have moved with a 'two steps forward and one step backward' intermittent motion, consistent with the precession observed both with the whole-field visualization and with the pressure measurements.

The *downstream* line of *negative bifurcation* appears to be caused by the presence of the lip in the exit plane of the nozzle. This lip was deduced by Nathan (1988) and by Vidakovic (1995) to be significant in determining the angle at which the jet leaves the nozzle.

The surface flow visualization provides complementary information to that available from the other techniques. It provides quantitative information about the distances to the lines of bifurcation and reveals the presence of an upstream negative bifurcation which is not readily apparent from the whole-field visualization. The presence of the upstream swirl is confirmed and its axial extent is determined. A comparison of the distances to the lines of bifurcation is given in § 4.3.

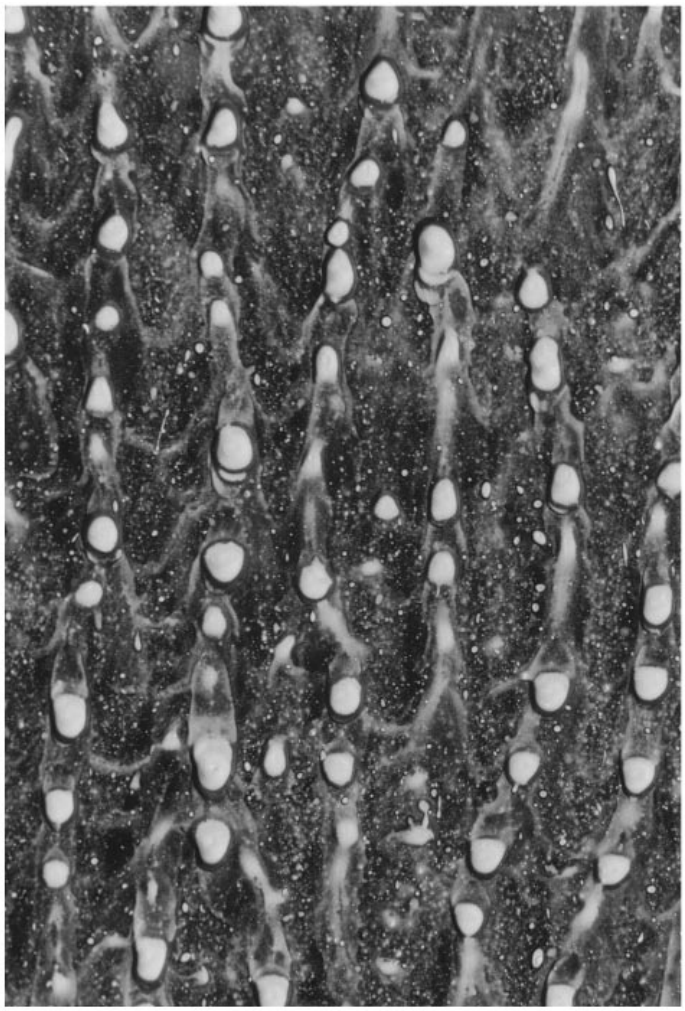

FIGURE 20. Enlargement of the surface flow image at the positive bifurcation line. Note that only the larger drops of the china clay mixture remain and that these do not appear to have moved very much during the drying process. (Conditions as specified for figure 17.)

4. Discussion

4.1. *Comparison with the Strouhal numbers in related flows*

It is worth comparing the Strouhal number associated with the large shear structures formed in the jet which enters the chamber, St_{s,d_1}, with that of the precession, St_{p,d_1}, as measured by total pressure probe 1. The data presented in figure 15 show that $0.0013 < St_{p,d} = f_p d/\bar{u} < 0.0017$. This value is two orders of magnitude lower than that associated with the shear-generated coherent structures in a jet identified by Crow & Champagne (1971). Crow & Champagne (1971) found the dimensionless frequency of these large 'puff'-like structures within the fully developed flow region of a free jet to be $St_{s,d} = f_s d/\bar{u} \approx 0.3$, where d is the exit diameter of the jet and f_s is the characteristic frequency of those shear stuctures. Likewise Hussain & Hasan (1983) measured the dominant frequency of structures in the shear layer around a potential core, when amplified through acoustic resonance, to be $0.3 < St_{s,d} = f_s d/\bar{u} < 0.8$. In

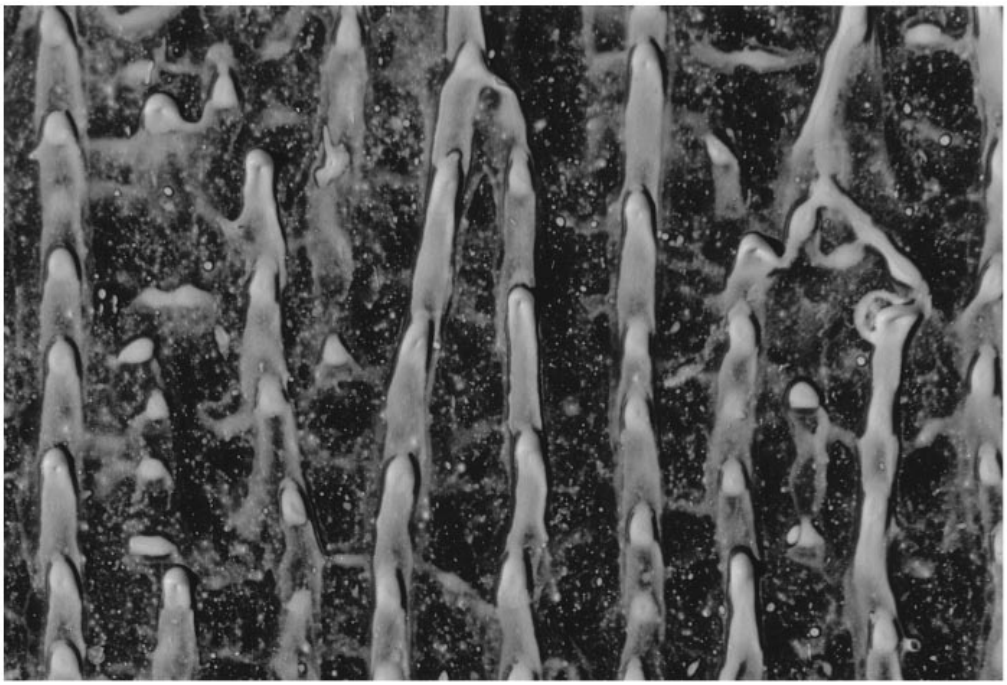

FIGURE 21. Enlargement of the surface pattern downstream from the positive bifurcation line. Again only the relatively large droplets have survived under the intense shear of the attached wall jet. (Conditions as specified for figure 17.)

the present case, the Strouhal number of the jet was measured both with the nozzle chamber removed and with the chamber attached and found to be $St_{s,d} \approx 0.5$ for $Re_1 = 53\,600$ and $St_{s,d} \approx 0.6$ for $Re_1 = 76\,700$. The measurements were performed with a hot-wire anemometer located at $x/d_1 = 3.0$ and $r/d_1 = 0.5$ in both conditions. The peak in the spectrum is much broader for the present orifice plate than that which occurs typically with a smooth contraction so that the frequency is only quoted to one significant figure. Nevertheless it is apparent that the spectra at this location are not influenced by the presence of the chamber. The weak dependence of $St_{s,d}$ on Re_1 is consistent with the findings of Becker & Massaro (1968). It is deduced that the most likely reason for the lower absolute values of $St_{s,d}$ in the present measurements compared to those of Becker & Massaro (1968) may be attributed to the different intial conditions (Becker used a smooth contraction at the nozzle exit).

That the Strouhal number of the dominant frequency in the present nozzle differs by two orders of magnitude from that related to either of the shear flow structures described above strongly suggests that the phenomena are distinctly different. The lower magnitude of the Strouhal number suggests that the frequency is associated with a larger motion of the jet as a whole, rather than with puff-like motions within the jet. Since it is the shear-generated puff structures which are associated with acoustic excitation (see e.g. Hill & Greene (1977) who measured the Strouhal number of the dominant frequency in an acoustically excited jet to be $0.25 < St_{s,d} = f_s d/\bar{u} < 0.65$) the result implies that the precession phenomenon is not acoustically induced. Further evidence to demonstrate that the present flow is not related to acoustic coupling is found in that the phenomenon occurs with the same $St_{p,d}$ when using either air or water, for which the Mach numbers differ by a factor of about 70, through the same

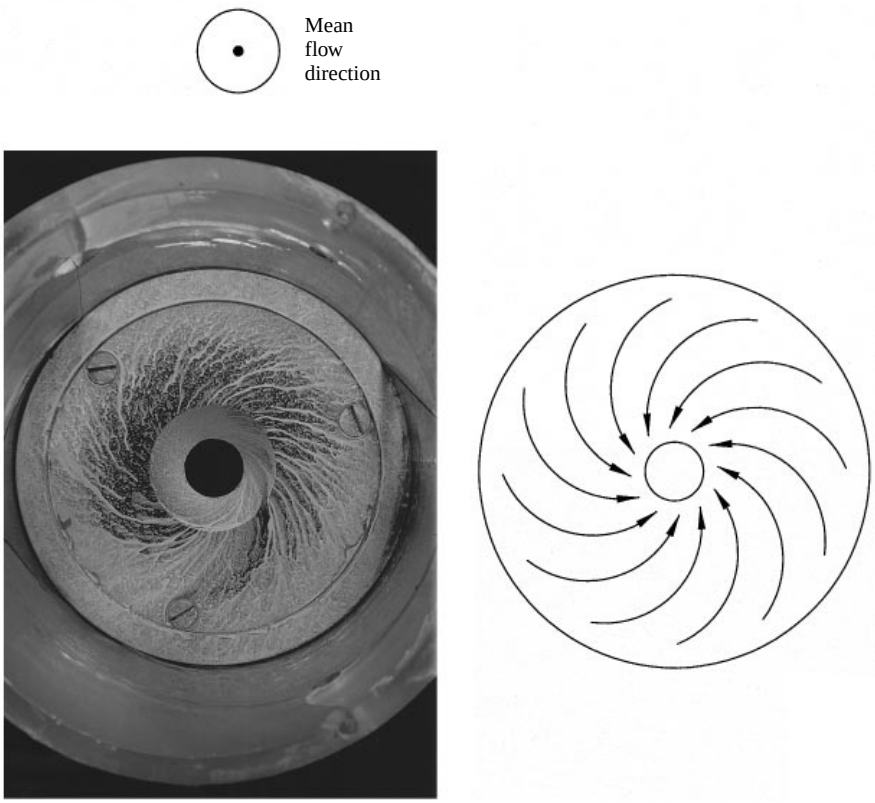

FIGURE 22. The china clay image formed on the surface of the upstream orifice plate. Here the strong, inwardly spiralling flow is clearly evident. (Conditions as specified for figure 17.)

nozzle or through different nozzles of similar geometric ratios (Nathan & Luxton 1992*a*).

While the Strouhal number of precession found in the present flow is very different from that of the puff structures found by Crow & Champagne (1971), it is remarkably similar to that found for a flapping jet in the planar fluidic oscillator investigated by Shakouchi (1981, 1989). In those experimental investigations Shakouchi determined that $St_{f,d} = f_f d/\bar{u} \approx 2 \times 10^{-3}$. The similarity between those Strouhal numbers and the present work further supports the interpretation that the dominant motion within the confines of the present axisymmetric chamber is associated with large-scale oscillations of the whole jet.

It is also interesting to compare the results from analogous studies of free planar jet flows which are stimulated to produce a large-scale flapping motion. Simmons *et al.* (1981) used a nozzle with an oscillating tip to produce a flapping, planar free jet and measured the dimensionless frequency of the flapping to be in the range $8 \times 10^{-4} < St_{f,d} = f_f d/\bar{u} < 5 \times 10^{-3}$. That the dimensionless frequency of the precession also lies within this range further supports the interpretation that the precession phenomenon is related to gross motions of the whole jet.

The large-scale motions associated with the precessing or flapping motion of a jet have been found in such a wide range of investigations that it is unrealistic to argue that such phenomena are intrinsically apparatus dependent. Even within the present investigation two entirely different, though geometrically similar, nozzles have

Source	Configuration	Re_1	d_1 (mm)	$\frac{2h+d_1}{d_1}$	x_{r1}/h	x_{r2}/h	x_{s1}/h	x_{s2}/h	Comments
Agarwal (1986)	Axisymmetric Orifice plate, long pipe air	30 000 to 70 000	45 to 60	1.6. to 1.2	9 to 12	–	1.5	–	time-mean flow symmetric
Abbot & Kline (1962)	Planar Back-Facing steps, in water	20 000 to 50 000	300 to 600	$\leqslant 1.5$ $\leqslant 1.5$ $\geqslant 1.5$ $\leqslant 5$	≈ 6 ≈ 6 ≈ 3	– 6 ≈ 9	1.2 1.2 ≈ 1	– 1.2 ≈ 3	single step double step asymmetric reattachment
Ouwa *et al.* (1981)	Planar B.F. steps, in water	250 to 400	4	5 10 20	≈ 5 ≈ 3 ≈ 2	≈ 12 ≈ 11 –	– – –	– – –	double step, jet-like flow
Pelfry & Liburdy (1986)	Planar wall jet, air	20 000	12.5	14	2.0	–	–	–	asymmetric reattachment
Present research	Axisymmetric PJ nozzle, in air	40 000 to 200 000	10 to 21	6.5 to 9.1	3.5	–	1.3	–	instantaneous asymmetric reattachment

TABLE 2. Comparison of the axial distances to lines of bifurcation observed for different reattaching flow configurations. Notation: d_1 is the inlet diameter or width, h is the step height, x_{r1} is the reattachment length when the reattachment is symmetric on either side of the exapnsion and also the shorter length when it is asymmetric x_{r2} is the longer of the reattachment lengths when the reattachment is asymmetric. Likewise x_{s1} and x_{s2} correspond to the distances to lines of negative bifurcation, or separation.

been used, one for the liquid flow visualization and one for the studies in air. The Strouhal number which characterizes the flow in the present apparatus, in which the inlet flow has a high degree of symmetry, has been found to agree well with that measured in other apparatus with less symmetric inlet flows (figure 15). This Strouhal number is two orders of magnitude lower than that which characterizes the shear generated 'puff' structures, identified by Crow & Champagne (1971), which emerges from the nozzle. Taken together, these observations suggest that minor mechanical asymmetries, which are inevitable in any configuration and can modify the structure of the inlet jet flow, are not significant in the generation of the observed precessing motions.

4.2. *Comparison of reattachment lengths in related flows*

It is instructive to compare the axial distances to the lines of bifurcation found in the present nozzle with those of related configurations reported by others. A summary of the results from these investigations is presented in table 2.

Eaton & Johnston (1981), in a review of reattaching flows, found that the reattachment length of a separated flow behind a backward facing step depends upon the initial boundary layer thickness and state (i.e. laminar or turbulent), the level of free-stream turbulence and the aspect ratio. The effect of expansion ratio, D/d, on the reattaching flow behind a sudden planar expansion for a given Reynolds number was examined by Abbot & Kline (1962). They found that the separated flow downstream from a planar, two-dimensional sudden expansion with turbulent entry is symmetrical in the mean only if the expansion ratio $D/d \leqslant 1.5$. For $D/d \geqslant 1.5$ the reattachment distance on one side of the expansion is longer than that on the other

due to the interaction between the two shear layers. As either the expansion ratio or the Reynolds number is increased, the degree of asymmetry in the flow increases, resulting in the formation of a third and then a fourth separation bubble (Armaly *et al.* 1983). Further increase of the expansion ratio to $D/d \geqslant 5$ results in a highly asymmetric reattachment of a jet-like flow, although this observation in long ducts appears to have been reported only with laminar conditions to date (Ouwa, Watanabe & Asawo 1981).

The reported trend for flow asymmetry to increase as the expansion ratio increases for planar configurations is qualitatively consistent with the present results in an axisymmetric configuration. However for an axisymmetric configuration the flow asymmetry implies the presence of pressure gradients in the azimuthal direction. While it is conceptually possible for a steady, asymmetric flow pattern to be established, in practice it is found that precession of that aysmmetric flow pattern occurs, suggesting that the steady flow pattern is highly unstable. It is also evident that once an azimuthal pressure field has been established it tends to dominate until a stronger transverse (diametral) gradient causes the jet to assume the (unstable) axial mode.

Agarwal (1986) investigated the flow through axisymmetric orifice plates with expansion ratios within the range investigated by Abbot & Kline (1962) in two dimensions. He found that the flow is symmetric on average and has a reattachment length, x_r, which depends weakly on the Reynolds number. The axial distance to the reattachment for the axial flow is in the range $9 \leqslant x_r/h \leqslant 12$, which is greater than that in the equivalent planar case which is $x_r/h \approx 6$ (table 2). Thus reattachment lengths of separated flows behind axisymmetric expansions are longer than those through planar configurations of the same diametral expansion ratio. However the reattachment lengths found by Agarwal (1986) are considerably longer than the $x_r/h \approx 3.5$ found in the axisymmetric expansion of the present nozzle. The expansion ratios which he investigated are also much smaller ($1.2 \leqslant D/d \leqslant 1.6$) consistent with the trends, found in the planar expansions, that dimensionless reattachment length decreases with increasing expansion ratio. Another significant difference between Agarwal's experimental arrangement and the present one is that the length of the downstream pipe, L, was large compared with its diameter, D.

The character of the jet-like reattachment observed in the whole-failed visualization of the present configuration is somewhat reminiscent of the reattachment of a wall jet. Here the axial distances to planes of bifurcation are compared with the planar wall jet investigated by Pelfry & Liburdy (1986). The latter measured the distance to the line of positive bifurcation to be $x_r/h = 2$. While this is somewhat shorter than the present value, $x_r/h \approx 3.5$ (table 2) it is of the same order. The comparison is also consistent with the trend that, for the same linear expansion ratio, a planar reattachment is shorter than is its axisymmetric analogue.

Summarizing the above discussion, the following trends can be seen in the data for flow behind a sudden expansion:

- The asymmetry of the reattaching flow increases with an increase in the expansion ratio. In a planar configuration the asymmetry is steady (unless each of the transverse dimensions of the jet is less than the corresponding chamber dimension, as in Shakouchi 1989). In an axisymmetric geometry the asymmetry is unsteady.
- The axial distance to the line of reattachment, when normalized by the step height, decreases with increasing expansion ratio.
- For a planar configuration the axial distance to the line of reattachment is shorter than that in an axisymmetric configuration of the same linear expansion ratio.

4.3. *Descriptive comments on the precessing flow field*

A descriptive interpretation of the character of the flow through the chamber has been deduced from various investigative techniques. Reference to the diagrammatic interpretation of the visualized flow, shown in figure 4, may be useful in interpreting the following comments.

As the turbulent jet enters the chamber through the upstream orifice, minor asymmetries in its local entrainment appetite, and hence in the local pressure field, are inevitable. Interaction with the confining chamber wall amplifies the local asymmetries in the pressure field causing the jet to move toward and reattach asymmetrically to the chamber wall. Unlike the behaviour in the analogous planar configuration, in which a bi-stable asymmetric reattachment is observed, in the present axisymmetric configuration reattachment is equally probable for all points around the inner circumference of the chamber. Hence any minor azimuthal variation in the pressure field, caused either by variations in the local flow structures in the reattaching jet or in the overall motion of the jet, will cause the point of reattachment to move. This is a positive feedback situation since any azimuthal movement of the reattachment point will immediately establish an azimuthal pressure field which will drive a self-sustaining precessing motion. At this point it should be noted that the net angular momentum of the flow entering the chamber through the upstream orifice is zero. Thus, to first order, the total angular momentum at any downstream plane should also be zero. It is logical that the angular momentum of the swirling flow is offset by an equal and opposite angular momentum of the whole reattaching jet.

The *reattached jet* (figure 4) continues in the downstream direction attached to one azimuthal section of the chamber wall as a wall jet, and exits the chamber from that same azimuthal location. The pressure in the chamber is sub-atmospheric, due to the entrainment of fluid by the jet within it, while the pressure outside the chamber is atmospheric. Thus the deflection of the wall jet toward the centreline by the lip at the exit plane is augmented by the strong pressure gradient at the exit of the chamber, whose direction is transverse relative to the deflected jet. The net effect is that the jet is deflected sharply across the nozzle axis as it leaves the chamber†. The sub-atmospheric pressure within the chamber also causes ambient fluid to be drawn into the chamber through that part of the exit plane not occupied by the jet. On the side of the chamber diametrically opposite the reattaching jet, the *recirculated fluid* moves upstream to the inlet end of the chamber where it slews to one side, so generating the *swirling flow*. A line of negative bifurcation results from the interaction between the swirling fluid and the recirculated fluid. The *swirling fluid* spirals radially inward, where it is entrained into the jet. It should be noted that, consistent with the conservation of angular momentum, dye visualization has shown that the rotational direction of the swirling flow is opposite to that of the precession (Nathan 1988).

5. Conclusions

A large-scale precessing flow instability within a cylindrical chamber downstream from a large sudden expansion has been investigated. This work is believed to be

† Vidakovic (1995) found, for a wall jet fixed at a given angular position in an axially profiled expanding chamber terminated by a lip at the exit plane, strong evidence that the separation vortex upstream from the lip loops back into the expansion and forms a 'necklace' around the wall jet. The associated pressure field greatly augments the deflection of the jet as it leaves the chamber. Whether or not such a vortex loop also exists in the present dynamic wall jet flow is unknown, but topologically it could exist.

the first in which great care has been taken to provide flow to the chamber which is symmetrical and well defined, and in which detailed measurements of both the inlet flow to the chamber and of the phenomenon itself have been reported.

The geometric configuration used in the present investigation consists of a cylindrical chamber with a large sudden expansion at its inlet with an expansion ratio, $D/d_1 = 6.4$, a relative length, $L/D = 2.6$, and a small contraction or lip at the exit plane. The jet entering the chamber was turbulent, with Reynolds numbers in the range $53\,000 < Re_1 < 134\,000$. The flow within the chamber has been shown to switch intermittently between two very different states, a highly asymmetric precessing jet (PJ) flow mode, which predominates in the present configuration, and a more symmetrical axial jet (AJ) mode. The focus of the present investigation is on the PJ mode because of its relevance to burner designs, in which application it has be shown elsewhere to provide the benefits of improved flame stability, lower NO_x emissions and, with natural gas as the fuel, increased flame radiation.

The broad characteristics of the two flow modes have been identified by use of water flow visualization. In addition, a surface flow visualization technique in air, which produces a time-averaged permanent record of the dominant flows in the chamber, has been used to quantify the axial distances to lines of surface flow bifurcation. Full-field visualization shows that, during the PJ mode, the jet entering the sudden expansion reattaches asymmetrically to the chamber wall and the reattachment point moves azimuthally around the wall. On reaching the exit plane of the nozzle, the jet does not wholly fill the exit plane and is deflected at a large angle across the nozzle axis by local pressure gradients associated with the presence of the exit lip and with the induction of ambient fluid into the nozzle chamber. This entire flow field precesses about the chamber axis in what may be described as a continuously unstable manner.

The axial distances to lines of bifurcation have been compared with those in several related flows. It appears that the distance to the dominant reattachment within the present chamber, $x_r/h \approx 3.5$, is more closely mirrored by the inherently asymmetric reattachment of a planar wall jet, $x_r/h \approx 2$, than by the reattachment associated with the generally symmetric flows entering a long cylindrical pipe through a smaller axisymmetric expansion ratio (i.e. $D/d_1 \leqslant 3.5$), for which $9 \leqslant x_r/h \leqslant 12$. This suggests that the degree of asymmetry in the instantaneous flow depends upon the expansion ratio. The observed reattachment distance is consistent with the trends described by other researchers using time-averaged techniques. That is, the dimensionless axial reattachment distance decreases with increasing expansion ratio and, for a given linear expansion ratio, planar reattachment distances tend to be shorter than those in axisymmetric configurations. This is logical as the volume of chamber fluid available for entrainment on the reattaching side of a jet is less for a two-dimensional flow than for an axisymmetric flow.

The main features of the present precessing flow have also been quantified by measurement of the fluctuating pressure field within the chamber using air as the working fluid. The Strouhal number of the precession is found to decrease slightly with increased Reynolds number and has been measured to be $St_{p,d_1} = f_p d_1/u_1 \approx 1.5 \times 10^{-3}$ (or $St_{p,D} = f_p \rho^{1/2} D^2/M^{1/2} \approx 0.07$). The magnitude of this Strouhal number is consistent with many previous measurements in a diverse range of axisymmetric apparatus demonstrating that the precessing flow phenomenon is relatively insensitive to changes in the inlet flow conditions and to minor apparatus-specific details. However previous results, conducted for conditions in which compressibility effects were negligible, found that St_p becomes independent of Re_1 at sufficiently high values

of Re_1. This suggests that the present weak dependence on Re_1 may be caused by compressibility effects.

The proportion of time that the flow spends in the PJ mode, $Prob(PJ)$, relative to the AJ mode has also been quantified for the present apparatus by observing a correlation between the flow mode and the wall pressure at the inlet to the chamber. A p.d.f. of this pressure shows a bi-modal distribution and the area under each hump provides a good estimate of the probability of that mode occurring. When the wall pressure corresponding to the saddle between the peaks in the bimodal p.d.f. is selected as the discriminating pressure, the probability of the PJ mode, $Prob(PJ)$, can be estimated and this estimate was found to increase slightly with Reynolds number. The present value of $Prob(PJ) \approx 95\%$ agrees quite well with other published data, although the techniques used to determine this value were different. A strong dependence of the $Prob(PJ)$ on chamber dimensions is also evident.

The frequency of precession is two orders of magnitude lower than the frequency of the dominant structures measured in the jet shear layer, consistent with data reported in the literature, suggesting that the two phenomena are distinctly different. The Strouhal number of the precession is, however, close to that of an analogous and larger-scale flapping motion in the planar jet investigated in considerable detail by Shakouchi (1989). It is noteworthy that minor rig-specific manufacturing imperfections or minor differences in the inlet velocity profile will manifest themselves in differences in the shear structures entering the chamber. The Strouhal numbers of such structures do not match of that of the precession. Furthermore the precessing phenomenon has been shown to occur within the same nozzle configuration using either air or water as the working fluid, for which the Mach numbers differ by a factor of about 70. These factors demonstrate that the phenomenon of precession described here does not derive from acoustic coupling. Taken together, the evidence suggests that the establishment of the observed continuously unstable precessing flow is dominated by the dimensions of the *downstream chamber*, and specifically upon the *expansion ratio*. The presence of a minor bias in the turbulence of the inlet flow has at most a minor effect on the details within the gross precessing motion.

The first author wishes to acknowledge the scholarship provided by the South Australian Energy Council during the early part of the research. The Australian Research Council and Adelaide Brighton Ltd have supported the second author through an Australian Postgraduate Research Award (Industry) and have directly supported the first and second authors, through its subsidiary Fuel & Combustion Technology Ltd., during the write-up phase of the work. Research grants from the Australian Research Council are also gratefully acknowledged. The understanding of the flow has evolved over many years and has benefited from numerous discussions with fluid dynamicists including P. Bradshaw, Deng Xue-Ying, P. V. Lanspeary and D. E. Ward during the early part of the work. The more recent reviewer's comments and those from colleagues R. M. Kelso, J. C. Mi, G. J. R. Newbold, D. S. Nobes, J. J. Parham, G. M. Schneider and N. L. Smith have significantly strengthened the final draft of the paper. All of these contributions are greatly appreciated.

REFERENCES

Abbot, D. E. & Kline, S. J. 1962 Experimental investigation of subsonic turbulent flow over single and double backward facing steps. *Trans. ASME: J. Basic Engng* **84**, 317–325.

Agarwal, N. K. 1986 Relationship between internal sound generation and characteristics of flow

in a region of flow separation due to disturbance of fully developed turbulent flow in a pipe. PhD thesis, Dept. Mech. Engng, The University of Adelaide.

Armaly, B. F., Durst, F., Perica, J. C. F. & Schonung, B. 1983 Experimental and theoretical investigation of backward facing step flow. *J. Fluid Mech.* **127**, 473–496.

Battaglia, F., Kulkarni, A. K., Feng, J. & Merkle, C. L. 1997 Simulation of planar flapping jets in confined channels. *AIAA Paper* 97-1992, pp. 1–11.

Becker, H. A. & Massaro, T. A. 1968 Vortex evolution in a round jet *J. Fluid Mech.* **31**, 435–448.

Bradshaw, P. 1970 *Experimental Fluid Mechanics*, 2nd Edn. Pergamon Press.

Crow, S. C. & Champagne, F. H. 1971 Orderly structure in jet turbulence. *J. Fluid Mech.* **483**, 547–591.

Dellenback, P. A., Metzger, D. E. & Neitzel, G. P. 1988 Measurements in a turbulent, swirling flow through an abrupt axi-symmetric expansion. *AIAA J.* **266**, 669–681.

Eaton, J. K. & Johnston, J. P. 1981 A review of research on subsonic turbulent flow reattachment. *AIAA J.* **19**, 1093–1100.

Hallett, W. L. H. & Gunther, R. 1984 Flow and mixing in swirling flow in a sudden expansion. *Can. J. Chem. Engng*, **62**, 149–155.

Hill, S. J. 1992 Characterisation of the flow fields produced by the enhanced mixing nozzle: a development towards high temperature and multi-phase applications. *Internal Rep.* Dept. Mech. Engng, The University of Adelaide.

Hill, S. J. 1998 Precessing flows in confined turbulent jets. PhD thesis (in preparation), Dept. Mech. Engng, The University of Adelaide.

Hill, S. J., Nathan, G. J. & Luxton, R. E. 1992 Precessing and axial flows following a sudden expansion in an axi-symmetric nozzle. *Eleventh Australasian Fluid Mechanics Conference, December, Hobart, Australia.*

Hill, S. J., Nathan, G. J. & Luxton, R. E. 1995 Precession in axi-symmetric confined jets, *Twelfth Australasian Fluid Mechanics Conference, December, Sydney, Australia.*

Hill, W. G., Jr. & Greene, P. R. 1977 Increased turbulent jet mixing rates obtained by self-excited acoustic cscillations *Trans. ASME I: J. Fluids Engng* **99**, 520–525.

Hornung, H. & Perry, A. E. 1984 Some aspects of three-dimensional separation, part I: Stream-surface bifurcations. *Z. Flugwiss. Weltramforsch.* **8**, 77–87.

Hunt, J. C. R., Abell, C. J., Peteraka, J. A. & Woo, H. 1978 Kinematic studies of the flows around free or surface-mounted obstacles; applying topology to flow visualisation. *J. Fluid Mech.* **86**, 179–200.

Hussain, A. K. M. F. & Hasan, M. A. Z. 1983 The 'whistler nozzle' phenomenon. *J. Fluid Mech.* **134**, 431–458.

Lipstein, N. J. 1962 Low velocity sudden expansion pipe flow. *ASHRAE J.* **4**, 43–47.

Luxton, R.E. & Nathan, G. J. 1989 A precessing asymmetric flow field in an abruptly expanding axi-symmetric duct, *Tenth Australasian Fluid Mechanics Conference, December, Melbourne, Australia*, vol. 2, pp. 11.29–11.33.

Luxton, R. E., Nathan, G. J. & Luminis Pty. Ltd. 1991 Mixing of fluids. *USA Letters Patent No. 5 060 867*, and other countries. Australian Patent Office, Application No. 16235/88.

Nathan, G. J. 1988 The enhanced mixing burner, PhD thesis, Dept. Mech. Engng, The University of Adelaide.

Nathan, G. J. & Luxton, R. E. 1988 A stable, un-premixed gas burner with infinite turn-down ratio. *First European Conf. Industrial Furnaces and Boilers, March, Lisbon, Portugal.*

Nathan, G. J. & Luxton, R. E. 1991 Flame stability and emission characteristics of the enhanced mixing burner. *Second European Conference on Industrial Furnaces and Boilers, April, Algarve, Portugal.*

Nathan, G. J. & Luxton, R. E. 1992*a* Mixing enhancement by a self-exciting, asymmetric precessing flow-field. In *Transport Phenomena in Heat and Mass Transfer*. (ed. J. A. Reizes), vol. 2, pp. 1297–1307. Elsevier.

Nathan, G. J. & Luxton, R. E. 1992*b* The flow field within an axi-symmetric nozzle utilising a large abrupt expansion. In *Recent Advances in Experimental Fluid Mechanics* (ed. F. G. Zhuang), pp. 527–532. Academic.

Nathan, G. J. & Luxton, R. E. 1997 Dye visualization of a precessing jet flow. *Album of Visualization*, No. 14, pp. 11–12.

Nathan, G. J., Luxton, R. E. & Smart, J. P. 1992 Reduced NO_x emissions and enhanced large

scale turbulence from a precessing jet burner. *24th Symp.* (*Intl*) *on Combustion*, pp. 1399–1405. The Combustion Institute.

NATHAN, G. J., TURNS, S. R. & BANDARU, R. V. 1996 The influence of jet precession on NO_x emissions and radiation from turbulent flames. *Combust. Sci. Technol.* **112**, 211–230.

NEWBOLD, G. J. R., NATHAN, G. J. & LUXTON, R. E. 1997 The large scale dynamic behavior of an unconfined precessing jet flame. *Combust. Sci. Technol.* **126**, 53.

OUWA, Y., WATANABE, M. & ASAWO, H. 1981 Flow visualisation of a two dimensional water jet in a rectangular channel. *Japan. J. Appl. Phys.* **20**, 243–247.

PELFREY, J. R. R. & LIBURDY, J. A. 1986 Mean flow characteristics of a turbulent offset jet. *Trans. ASME* I: *J. Fluids Engng* **108**, 82–88.

PIATT, M. & VIETS, H. 1979 Conditioned sampling in an unsteady jet *AIAA Paper* 79-1857, pp. 1–8.

SHAKOUCHI, T. 1981 An experimental study on the cavity type fluidic oscillator. *Res. Rep. Fac. Engng Mie. Univ.* **6**, 1–13.

SHAKOUCHI, T. 1989 A new fluidic oscillator, flowmeter, without control port and feedback loop. *J. Dyn. Systems, Measurement Control* **111**, 535–539.

SIMMONS, J. M., LAI, J. C. S. & PLATZER, M. F. 1981 Jet excitation by an oscillating vane. *AIAA J.* **19**, 673–676.

TOBAK, M. & PEAKE, D. J. 1979 Topology of two-dimensional and three-dimensional separated flows. *AIAA Paper*, 79-1480, pp. 1–29.

VIDAKOVIC, S. S. 1995 *Fluid mechanics of deflected jets.* PhD thesis, Dept. Mech. Engng, The University of Adelaide.

WANG, K. C. 1974 Boundary layer over a blunt body at high incidence with an open-type of separation. *Proc. R. Soc. Lond.* A, **340**, 33–55.